

**REPORT ON A HELICOPTER-BORNE
VERSATILE TIME DOMAIN ELECTROMAGNETIC (VTEM^{plus}) AND
HORIZONTAL MAGNETIC GRADIOMETER GEOPHYSICAL SURVEY**

Ermatinger North & Ermatinger South Properties

Sudbury, Ontario

For:

Wallbridge Mining Company Limited

Geotech Ltd.

245 Industrial Parkway North

Aurora, Ont., CANADA, L4G 4C4

Tel: 1.905.841.5004

Fax: 1.905.841.0611

www.geotech.ca

Email: info@geotech.ca

Survey flown during May & June, 2011

Project 11117

July, 2011

TABLE OF CONTENTS

Executive Summary	ii
1. INTRODUCTION	1
1.1 General Considerations.....	1
1.2 Survey and System Specifications.....	2
1.3 Topographic Relief and Cultural Features.....	3
2. DATA ACQUISITION	4
2.1 Survey Area.....	4
2.2 Survey Operations.....	4
2.3 Flight Specifications.....	6
2.4 Aircraft and Equipment.....	6
2.4.1 Survey Aircraft.....	6
2.4.2 Electromagnetic System.....	6
2.4.3 Horizontal Magnetic Gradiometer.....	10
2.4.4 Radar Altimeter.....	10
2.4.5 GPS Navigation System.....	10
2.4.6 Digital Acquisition System.....	10
2.5 Base Station.....	11
3. PERSONNEL	12
4. DATA PROCESSING AND PRESENTATION	13
4.1 Flight Path.....	13
4.2 Electromagnetic Data.....	13
4.3 Magnetic Data.....	15
5. DELIVERABLES	16
5.1 Survey Report.....	16
5.2 Maps.....	16
5.3 Digital Data.....	16
6. CONCLUSIONS AND RECOMMENDATIONS	20
6.1 Conclusions.....	20
6.2 Recommendations.....	20

LIST OF FIGURES

Figure 1 - Property Location.....	1
Figure 2 – survey area location on Google Earth.....	2
Figure 3 – Flight path over a Google Earth Image.....	3
Figure 4 - VTEM ^{plus} Configuration, with magnetometer.....	7
Figure 5 - VTEM Waveform & Sample Times.....	7
Figure 6 – VTEM ^{plus} System Configuration.....	9
Figure 7 - Z, X and Fraser filtered X (FFx) components for “thin” target.....	14

LIST OF TABLES

Table 1 - Survey Specifications.....	4
Table 2 - Survey schedule.....	4
Table 3 - Decay Sampling Scheme.....	8
Table 4 - Acquisition Sampling Rates.....	10
Table 5 - Geosoft GDB Data Format.....	17

APPENDICES

A. Survey Location Maps.....	
B. Survey Block Coordinates.....	
C. VTEM Waveform.....	
D. Geophysical Maps.....	
E. Generalized Modelling Results of the VTEM System.....	
F. TAU Analysis.....	
G. TEM Resistivity Depth Imaging (RDI).....	

REPORT ON A HELICOPTER-BORNE VERSATILE TIME DOMAIN ELECTROMAGNETIC (VTEM^{plus}) and HORIZONTAL MAGNETIC GRADIOMETER GEOPHYSICAL SURVEY

Ermatinger North & Ermatinger South Properties
Sudbury, Ontario

Executive Summary

From May 4th to June 6th, 2011 Geotech Ltd. carried out a helicopter-borne geophysical survey over the Ermatinger North and Ermatinger South properties situated approximately 50 kilometres west of Sudbury, Ontario, Canada.

Principal geophysical sensors included a versatile time domain electromagnetic (VTEM^{plus}) system, and horizontal magnetic gradiometer. Ancillary equipment included a GPS navigation system and a radar altimeter. A total of 1016.2 line-kilometres of geophysical data were acquired during the survey.

In-field data quality assurance and preliminary processing were carried out on a daily basis during the acquisition phase. Preliminary and final data processing, including generation of final digital data and map products were undertaken from the office of Geotech Ltd. in Aurora, Ontario.

The processed survey results are presented as the following maps:

- Total Magnetic Intensity (TMI)
- Total Horizontal Gradient of TMI
- dB/dt Z Component Channel
- Tilt Derivative of TMI
- Electromagnetic stacked profiles of the B-field Z Component
- Electromagnetic stacked profiles of the dB/dt Z Component
- Calculated Time Constant (TAU) from dB/dt Z Component

Digital data includes all electromagnetic and magnetic products, plus ancillary data including the waveform.

The survey report describes the procedures for data acquisition, processing, final image presentation and the specifications for the digital data set.

1. INTRODUCTION

1.1 General Considerations

Geotech Ltd. performed a helicopter-borne geophysical survey over the Ermatinger North and Ermatinger South Properties located approximately 50km west of Sudbury, Ontario (Figure 1 & 2).

Dave Smith represented Wallbridge Mining Company Limited during the data acquisition and data processing phases of this project.

The geophysical surveys consisted of helicopter borne EM using the versatile time-domain electromagnetic (VTEM^{plus}) system with Z and X component measurements and horizontal magnetic gradiometer using two cesium magnetometers. A total of 1016.2 line-km of geophysical data were acquired during the survey.

The crew was based out of Sudbury, Ontario (Figure 2) for the acquisition phase of the survey. Survey flying started on May 4th and was completed on June 6th, 2011.

Data quality control and quality assurance, and preliminary data processing were carried out on a daily basis during the acquisition phase of the project. Final data processing followed immediately after the end of the survey. Final reporting, data presentation and archiving were completed from the Aurora office of Geotech Ltd. in July, 2011.

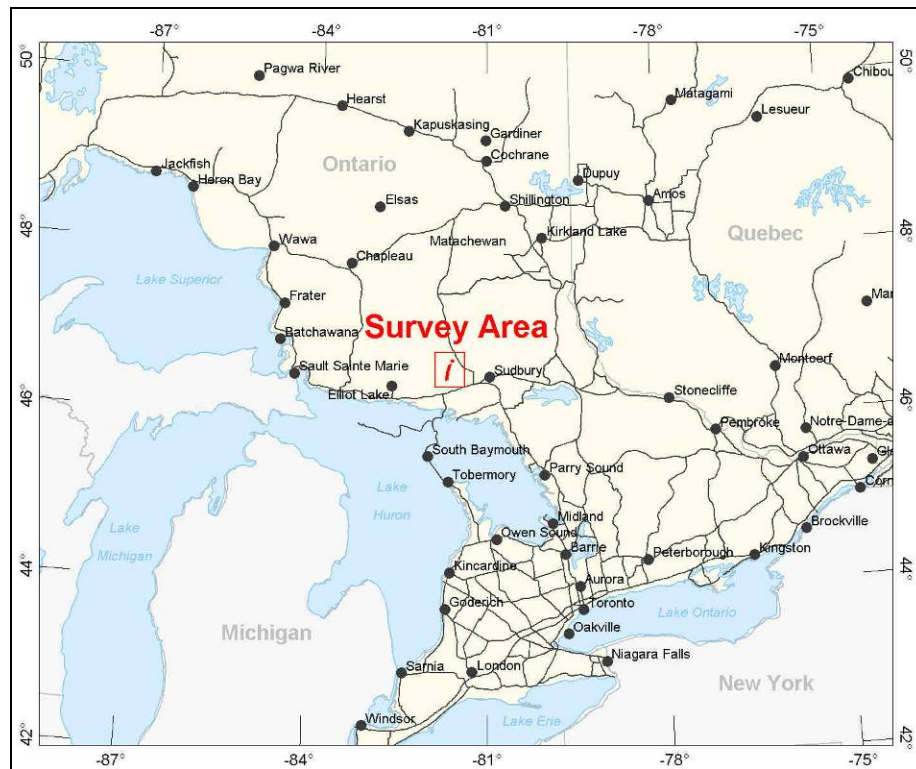


Figure 1 - Property Location

1.2 Survey and System Specifications

The survey area is located approximately 50 kilometres west of Sudbury, Ontario (Figure 2).

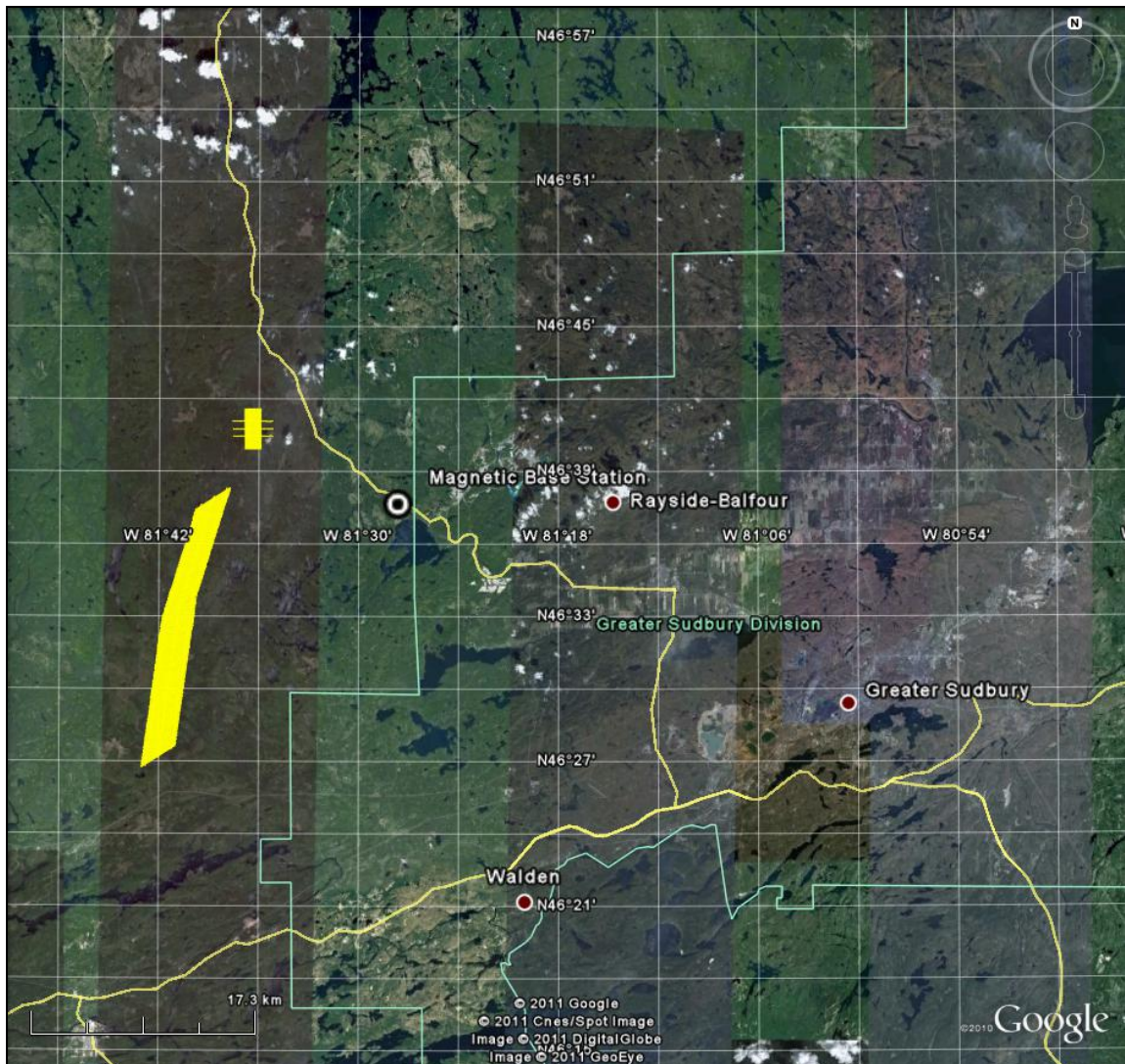


Figure 2 – Survey area location on Google Earth

The Ermatinger South blocks were flown in a northeast to southwest ($N 58^{\circ} E$ azimuth) and the Ermatinger North block was flown in an east to west ($N 90^{\circ} E$ azimuth) direction with traverse line spacing's of 50 metres as depicted in Figure 3. Tie lines were flown perpendicular to the traverse lines. For more detailed information on the flight spacing and direction see Table 1.

1.3 Topographic Relief and Cultural Features

Topographically, the blocks exhibit a shallow relief with elevations ranging from 290 to 431 metres above mean sea level over an area of 50 square kilometres (Figure 3). There are various rivers and streams running through the survey area which connect various lakes and wetlands. Roads and trails can also be found throughout the survey area. Special care is recommended in identifying any potential cultural features from other sources that might be recorded in the data.

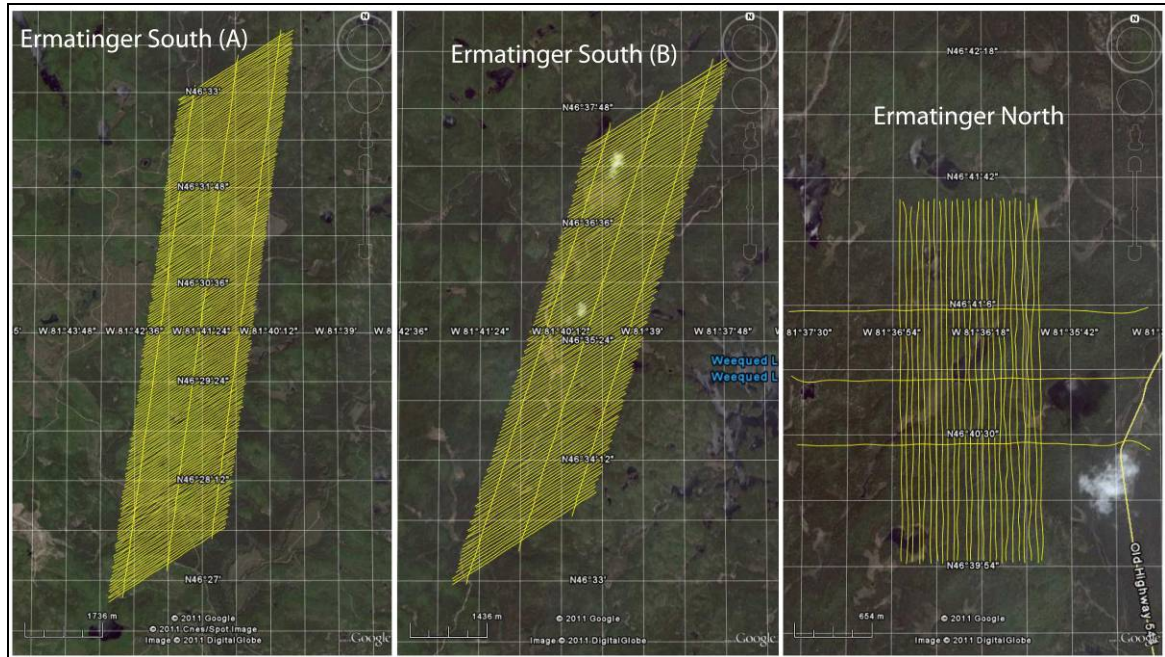


Figure 3 – Flight path over a Google Earth Image.

The survey area is covered by numerous Ontario mining claims, which are shown in Appendix A, and are plotted on all maps. The survey area is covered by NTS (National Topographic Survey) of Canada sheets 041I12 and 041I05.

2. DATA ACQUISITION

2.1 Survey Area

The survey block (see Figure 3 and Appendix A) and general flight specifications are as follows:

Table 1 - Survey Specifications

Survey block	Traverse Line spacing (m)	Area (Km ²)	Planned ¹ Line-km	Actual Line-km	Flight direction	Line numbers
Ermatinger North	Traverse: 50	4	84	86.9	N 90° E / N 270° E	L5000 – L5240
	Tie: 550 & 600				N 0° E / N 180° E	T6000 – T6020
Ermatinger South (A)	Traverse: 50	28	566.7	592.4	N 58° E / N 238° E	L1000 – L2760
	Tie: 800				N 8° E / N 188° E	T4000 – T4020
Ermatinger South (B)	Traverse: 50	18	365.5	384.1	N 58° E / N 238° E	L2770 – L3890
	Tie: 750				N 17° E / N 197° E	T4030 – T4050
TOTAL		50	1016.2	1063.4		

Survey block boundaries co-ordinates are provided in Appendix B.

2.2 Survey Operations

Survey operations were based out of Sudbury, Ontario from May 4th, 2011 to June 6th, 2011. The following table shows the timing of the flying.

Table 2 - Survey schedule

Date	Flight #	Block	Crew location	Comments
4-May-11	1	Erm. North	Sudbury, ON	limited production due to weather
5-May-11	2,3,4	Erm. North	Sudbury, ON	production
6-May-11		Erm. South (A)	Sudbury, ON	No production due to weather
7-May-11	5,6	Erm. South (A)	Sudbury, ON	limited production due to weather
8-May-11			Sudbury, ON	No production due to system maintenance
9-May-11	7	Erm. South (A)	Sudbury, ON	limited production due to system maintenance
10-May-11			Sudbury, ON	No production due to system maintenance
11-May-11	8,9	Erm. South (A)	Sudbury, ON	production
12-May-11			Sudbury, ON	No production due to system maintenance
13-May-11			Sudbury, ON	No production due to weather
14-May-11			Sudbury, ON	No production due to weather
15-May-11			Sudbury, ON	No production due to weather
16-May-11			Sudbury, ON	No production due to weather
17-May-11	10	Erm. South (A)	Sudbury, ON	Production aborted due to technical issues
18-May-11			Sudbury, ON	Production aborted due to technical issues
19-May-11			Sudbury, ON	Production aborted due to technical issues
20-May-11			Sudbury, ON	Technical issues

¹ Note: Actual Line kilometres represent the total line kilometres in the final database. These line-km normally exceed the Planned line-km, as indicated in the survey NAV files.

21-May-11			Sudbury, ON	Technical issues
22-May-11			Sudbury, ON	Technical issues
23-May-11			Sudbury, ON	Technical issues
24-May-11			Sudbury, ON	Technical issues
25-May-11			Sudbury, ON	Technical issues
26-May-11			Sudbury, ON	System testing
27-May-11			Sudbury, ON	System testing
28-May-11			Sudbury, ON	System testing
29-May-11			Sudbury, ON	System testing
30-May-11	11,12	Erm. South (A)	Sudbury, ON	limited production due to testing
31-May-11			Sudbury, ON	System testing
1-Jun-11	13	Erm. South (B)	Sudbury, ON	limited production due to testing
2-Jun-11	14	Erm. South (B)	Sudbury, ON	limited production due to testing
3-Jun-11	15,16,17	Erm. South (B)	Sudbury, ON	production
4-Jun-11			Sudbury, ON	No production due to weather
5-Jun-11	18,19,20	Erm. South (B)	Sudbury, ON	production
6-Jun-11	21	Erm. South (B)	Sudbury, ON	Remaining kms flown – flying complete

2.3 Flight Specifications

During the survey the helicopter was maintained at a mean altitude of 83 metres above the ground with a nominal survey speed of 80 km/hour. This allowed for a nominal EM bird terrain clearance of 48 metres and a magnetic sensor clearance of 70 metres.

The on board operator was responsible for monitoring the system integrity. He also maintained a detailed flight log during the survey, tracking the times of the flight as well as any unusual geophysical or topographic features.

On return of the aircrew to the base camp the survey data was transferred from a compact flash card (PCMCIA) to the data processing computer. The data were then uploaded via ftp to the Geotech office in Aurora for daily quality assurance and quality control by qualified personnel.

2.4 Aircraft and Equipment

2.4.1 Survey Aircraft

The survey was flown using a Eurocopter Aerospatiale (Astar) 350 B3 helicopter, registration C-GEOC. The helicopter is owned and operated by Geotech Aviation. Installation of the geophysical and ancillary equipment was carried out by a Geotech Ltd crew.

2.4.2 Electromagnetic System

The electromagnetic system was a Geotech Time Domain EM (VTEM^{plus}) system. The configuration is as indicated in Figure 4.

The VTEM Receiver and transmitter coils were in concentric-coplanar and Z-direction oriented configuration. The receiver system for the project also included a coincident-coaxial X-direction coil to measure the in-line dB/dt and calculate B-Field responses. The EM bird was towed at a mean distance of 35 metres below the aircraft as shown in Figure 4 and Figure 6. The receiver decay recording scheme is shown diagrammatically in Figure 5.

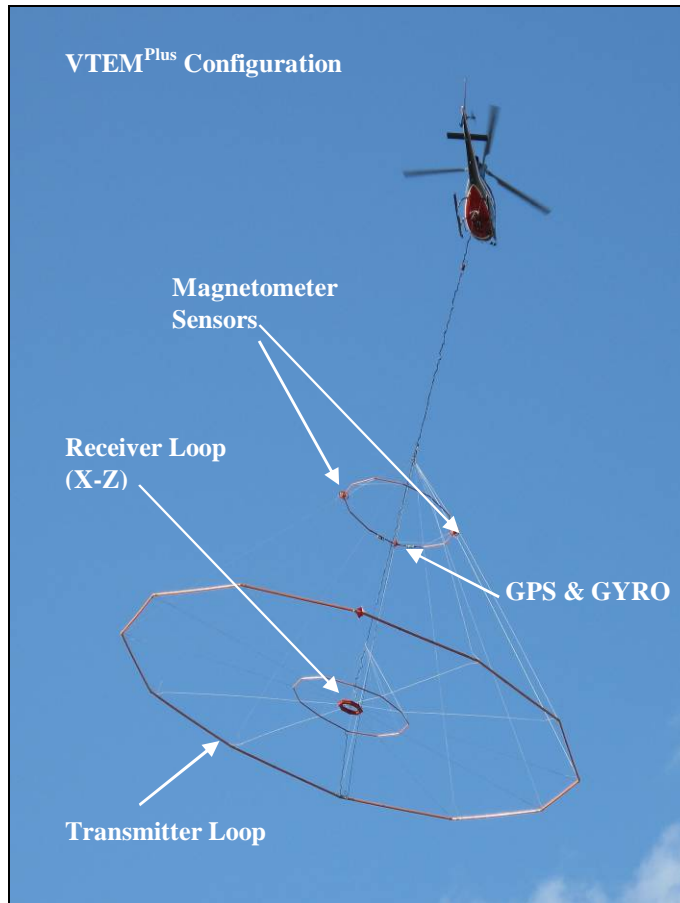


Figure 4 - VTEM^{plus} Configuration, with magnetometer.

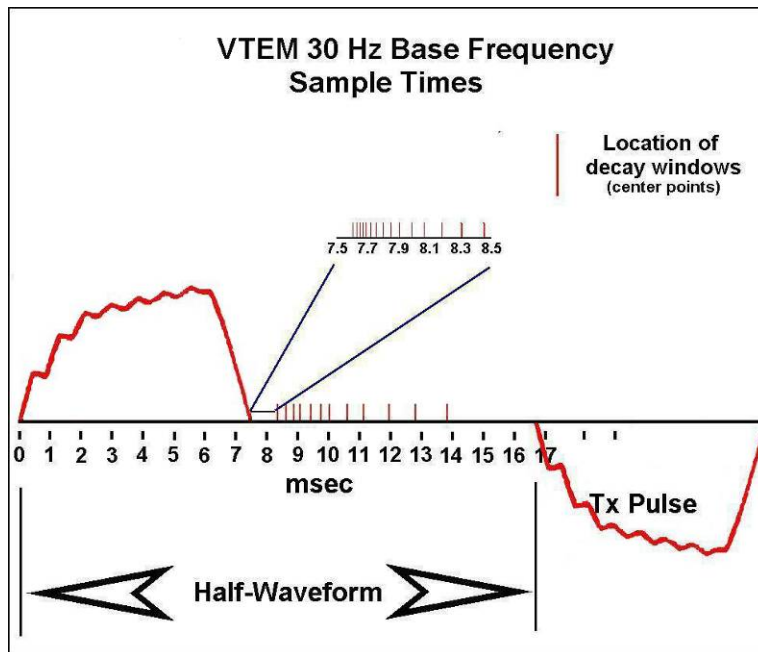


Figure 5 - VTEM Waveform & Sample Times

The VTEM decay sampling scheme is shown in Table 3 below. Thirty-two time measurement gates were used for the final data processing in the range from 96 to 7036 μ sec.

Table 3 - Decay Sampling Scheme

VTEM Decay Sampling Scheme				
Index	Middle	Start	End	Window
Microseconds				
14	96	90	103	13
15	110	103	118	15
16	126	118	136	18
17	145	136	156	20
18	167	156	179	23
19	192	179	206	27
20	220	206	236	30
21	253	236	271	35
22	290	271	312	40
23	333	312	358	46
24	383	358	411	53
25	440	411	472	61
26	505	472	543	70
27	580	543	623	81
28	667	623	716	93
29	766	716	823	107
30	880	823	945	122
31	1,010	945	1,086	141
32	1,161	1,086	1,247	161
33	1,333	1,247	1,432	185
34	1,531	1,432	1,646	214
35	1,760	1,646	1,891	245
36	2,021	1,891	2,172	281
37	2,323	2,172	2,495	323
38	2,667	2,495	2,865	370
39	3,063	2,865	3,292	427
40	3,521	3,292	3,781	490
41	4,042	3,781	4,341	560
42	4,641	4,341	4,987	646
43	5,333	4,987	5,729	742
44	6,125	5,729	6,581	852
45	7,036	6,581	7,560	979

VTEM system parameters:

Transmitter Section

- Transmitter coil diameter: 26 m
- Number of turns: 4
- Transmitter base frequency: 30 Hz
- Peak current: 167 A
- Pulse width: 7.21 ms
- Duty cycle: 43 %
- Wave form shape: trapezoid
- Peak dipole moment: 354,660 nIA
- Nominal EM Bird terrain clearance: 48 metres above the ground
- Effective coil area: 2123 m²

Receiver Section

X-Coil

- X Coil diameter: 0.32 m
- Number of turns: 245
- Effective coil area: 19.69 m²

Z-Coil

- Z-Coil coil diameter: 1.2 m
- Number of turns: 100
- Effective coil area: 113.04 m²

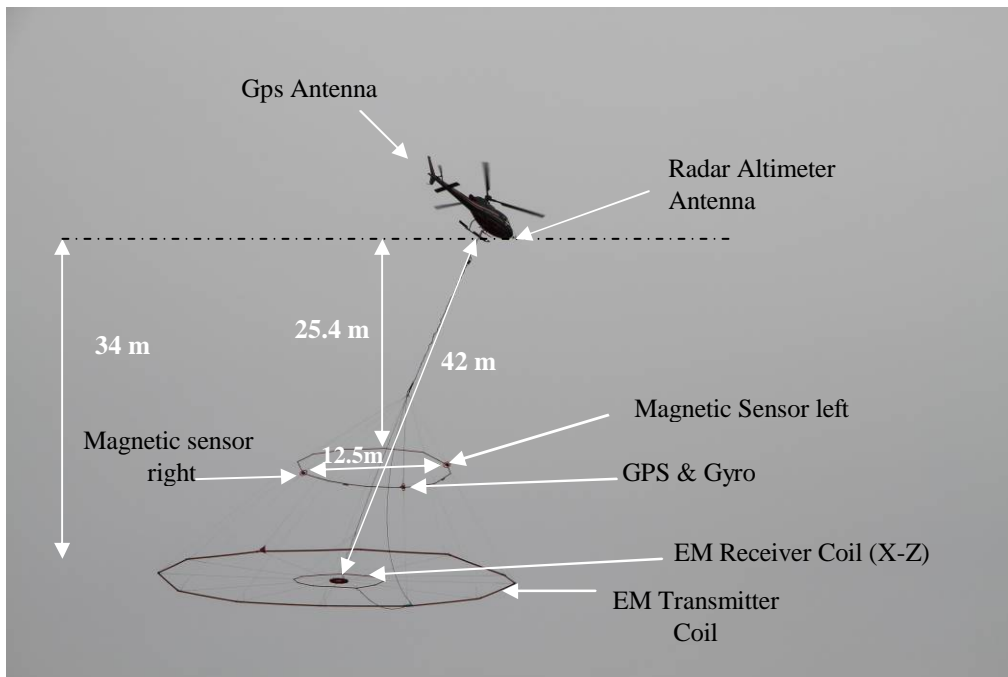


Figure 6 – VTEM^{plus} System Configuration

2.4.3 Horizontal Magnetic Gradiometer

The horizontal magnetic gradiometer consists of two Geometrics split-beam field magnetic sensors with a sampling interval of 0.1 seconds. These sensors are mounted 12.5 metres apart on a separate bird, 10 metres above the EM bird. A GPS antenna and Gyro is installed to accurately record the tilt and position of the magnetic gradiomag bird.

2.4.4 Radar Altimeter

A Terra TRA 3000/TRI 40 radar altimeter was used to record terrain clearance. The antenna was mounted beneath the bubble of the helicopter cockpit (Figure 6).

2.4.5 GPS Navigation System

The navigation system used was a Geotech PC104 based navigation system utilizing a NovAtel's CDGPS (Canada-Wide Differential Global Positioning System Correction Service) enable OEM4-G2-3151W GPS receiver, Geotech navigate software, a full screen display with controls in front of the pilot to direct the flight and an NovAtel GPS antenna mounted on the helicopter tail (Figure 6). As many as 11 GPS and two CDGPS satellites may be monitored at any one time. The positional accuracy or circular error probability (CEP) is 1.8 m, with CDGPS active, it is 1.0 m. The co-ordinates of the block were set-up prior to the survey and the information was fed into the airborne navigation system.

2.4.6 Digital Acquisition System

A Geotech data acquisition system recorded the digital survey data on an internal compact flash card. Data is displayed on an LCD screen as traces to allow the operator to monitor the integrity of the system. The data type and sampling interval as provided in Table 4.

Table 4 - Acquisition Sampling Rates

DATA TYPE	SAMPLING
TDEM	0.1 sec
Magnetometer	0.1 sec
GPS Position	0.2 sec
Radar Altimeter	0.2 sec

2.5 Base Station

A combined magnetometer/GPS base station was utilized on this project. A Geometrics Cesium vapour magnetometer was used as a magnetic sensor with a sensitivity of 0.001 nT. The base station was recording the magnetic field together with the GPS time at 1 Hz on a base station computer.

The base station magnetometer sensor was installed in a wooded near the crew's lodgings (46°37'43.64"N, 81° 27'32.00"W); away from electric transmission lines and moving ferrous objects such as motor vehicles. The base station data were backed-up to the data processing computer at the end of each survey day.

3. PERSONNEL

The following Geotech Ltd. personnel were involved in the project.

Field:

Project Manager:	Adrian Sarmasag (office)
Data QA/QC:	Neil Fiset (office)
Crew chief:	Ioan Serbu/Calin Cosma
System Operators:	Michael Altman/John West-Fiset

The survey pilot and the mechanical engineer were employed directly by the helicopter operator – Geotech Aviation.

Pilot:	Geo Rawlings
Mechanical Engineers:	Oleg Babisin/James Ni

Office:

Preliminary Data Processing:	Neil Fiset
Final Data Processing:	Karl Kwan
Final Data QA/QC:	Alexander Prikhodko
Reporting/Mapping:	Kyle Orłowski

Data acquisition phase was carried out under the supervision of Andrei Bagrianski, P. Geo, Chief Operating Officer. Processing phase was carried out under the supervision of Alexander Prikhodko, P. Geo, Senior Geophysicist, VTEM Interpretation Supervisor. The customer relations were looked after by Jennifer Stefano

4. DATA PROCESSING AND PRESENTATION

Data compilation and processing were carried out by the application of Geosoft OASIS Montaj and programs proprietary to Geotech Ltd.

4.1 Flight Path

The flight path, recorded by the acquisition program as WGS 84 latitude/longitude, was converted into the NAD 27 Datum, UTM Zone 17 North coordinate system in Oasis Montaj.

The flight path was drawn using linear interpolation between x, y positions from the navigation system. Positions are updated every second and expressed as UTM easting's (x) and UTM northing's (y).

4.2 Electromagnetic Data

A three stage digital filtering process was used to reject major spheric events and to reduce noise levels. Local spheric activity can produce sharp, large amplitude events that cannot be removed by conventional filtering procedures. Smoothing or stacking will reduce their amplitude but leave a broader residual response that can be confused with geological phenomena. To avoid this possibility, a computer algorithm searches out and rejects the major spheric events.

The signal to noise ratio was further improved by the application of a low pass linear digital filter. This filter has zero phase shift which prevents any lag or peak displacement from occurring, and it suppresses only variations with a wavelength less than about 1 second or 15 metres. This filter is a symmetrical 1 sec linear filter.

The results are presented as stacked profiles of EM voltages for the time gates, in linear - logarithmic scale for the B-field Z component and dB/dt responses in the Z and X components. dB/dt Z component time channel recorded at 0.167 milliseconds after the termination of the impulse is also presented as contour color image. Fraser Filter X component is also presented as a colour image. Calculated Time Constant (TAU) with anomaly contours of Calculated Vertical Derivative of TMI is presented in Appendix D and F. Tau was calculated using noise level of 0.025 for dB/dt and 0.007 for B-Field. Resistivity Depth Image (RDI) is also presented in Appendix D and G.

VTEM has two receiver coil orientations. Z-axis coil is oriented parallel to the transmitter coil axis and both are horizontal to the ground. The X-axis coil is oriented parallel to the ground and along the line-of-flight. This combined two coil configuration provides information on the position, depth, dip and thickness of a conductor. Generalized modeling results of VTEM data, are shown in Appendix E.

In general X-component data produce cross-over type anomalies: from “+ to –” in flight direction of flight for “thin” sub vertical targets and from “- to +” in direction of flight for “thick” targets. Z component data produce double peak type anomalies for “thin” sub vertical targets and single peak for “thick” targets.

The limits and change-over of “thin-thick” depends on dimensions of a TEM system. For example, for VTEM-26 the border corresponds to diameter of the system (Appendix E, Fig.E-16).

Because of X component polarity is under line-of-flight, convolution Fraser Filter (Figure 7) is applied to X component data to represent axes of conductors in the form of grid map. In this case positive FF anomalies always correspond to “plus-to-minus” X data crossovers independent of the flight direction.

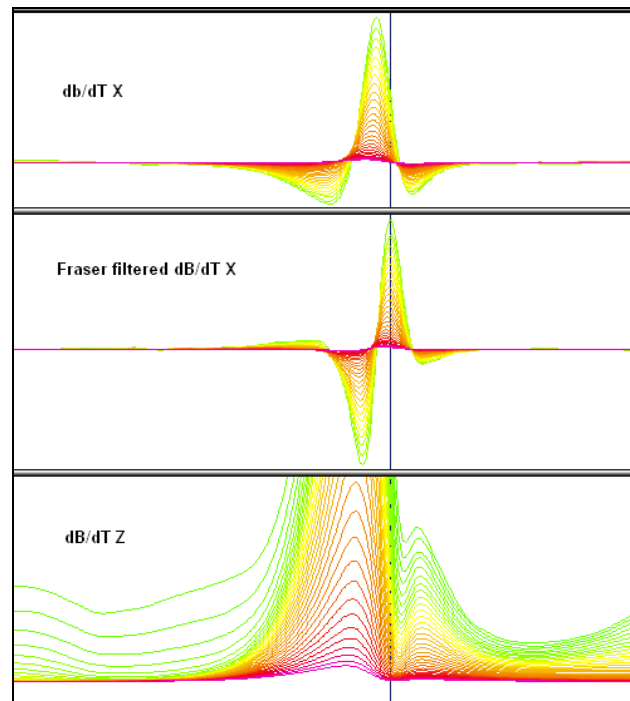


Figure 7 - Z, X and Fraser filtered X (FFx) components for “thin” target

Graphical representations of the VTEM transmitter input current and the output voltage of the receiver coil are shown in Appendix C.

4.3 Horizontal Magnetic Gradiometer Data

The horizontal gradients data from the VTEM^{plus} are measured by two magnetometers 12.5 m apart on an independent bird mounted 10m above the VTEM loop. A GPS and a Gyro help to determine the positions and orientations of the magnetometers. The data from the two magnetometers are corrected for position and orientation variations, as well as for the diurnal variations using the base station data.

The position of the centre of the horizontal magnetic gradiometer bird is calculated from the GPS utilizing in-house processing tool in Geosoft. Following that total magnetic intensity is calculated at the center of the bird by calculating the mean values from both sensors. In addition to the total intensity advanced processing is done to calculate the in-line and cross-line (or lateral) horizontal gradient which enhance the understanding of magnetic targets. The in-line (longitudinal) horizontal gradient is calculated from the difference of two consecutive total magnetic field readings divided by the distance along the flight line direction, while the cross-line (lateral) horizontal magnetic gradient is calculated from the difference in the magnetic readings from both magnetic sensors divided by their horizontal separation.

Two advanced magnetic derivative products, the total horizontal derivative (THDR), and tilt angle derivative and are also created. The total horizontal derivative or gradient is also called the analytic signal, is defined as:

$THDR = \sqrt{H_x^2 + H_y^2}$, where H_x and H_y are cross-line and in-line horizontal gradients.

The tilt angle derivative (TDR) is defined as:

$TDR = \arctan(V_z/THDR)$, where THDR is the total horizontal derivative, and V_z is the vertical derivative.

Measured cross-line gradients can help to enhance cross-line linear features during gridding.

5. DELIVERABLES

5.1 Survey Report

The survey report describes the data acquisition, processing, and final presentation of the survey results. The survey report is provided in two paper copies and digitally in PDF format.

5.2 Maps

Final maps were produced at scale of 1:10,000 for best representation of the survey size and line spacing. The coordinate/projection system used was NAD 27 Datum, UTM Zone 17 North. All maps show the mining claims, flight path trace and topographic data; latitude and longitude are also noted on maps.

The preliminary and final results of the survey are presented as EM profiles, a late-time gate gridded EM channel, and a colour magnetic TMI contour map. The following maps are presented on paper;

- VTEM dB/dt profiles Z Component, Time Gates 0.126 – 4.042 ms in linear – logarithmic scale.
- VTEM dB/dt early time Z Component Channel 18, Time Gate 0.167 ms colour image.
- VTEM B-Field profiles Z Component, Time Gates 0.220 – 7.036 ms in linear – logarithmic scale.
- Total Magnetic Intensity (TMI) colour image and contours.
- VTEM dB/dt Calculated Time Constant (TAU) with contours of anomaly areas of the Calculated Vertical Derivative of TMI
- Total Horizontal Gradient of TMI

5.3 Digital Data

- Two copies of the data and maps on DVD were prepared to accompany the report. Each DVD contains a digital file of the line data in GDB Geosoft Montaj format as well as the maps in Geosoft Montaj Map and PDF format.
- DVD structure.

Data	contains databases, grids and maps, as described below.
Report	contains a copy of the report and appendices in PDF format.

Databases in Geosoft GDB format, containing the channels listed in Table 5.

Table 5 - Geosoft GDB Data Format

Channel name	Units	Description
X:	metres	UTM Easting NAD 27 Zone 17 North
Y:	metres	UTM Northing NAD 27 Zone 17 North
Longitude:	Decimal Degrees	NAD 27 Longitude data
Latitude:	Decimal Degrees	NAD 27 Latitude data
Z:	metres	GPS antenna elevation (above Geoid)
Radar:	metres	helicopter terrain clearance from radar altimeter
Radarb:	metres	Calculated EM bird terrain clearance from radar altimeter
DEM:	metres	Digital Elevation Model
G2time:	Seconds of the day	GPS time
Mag1_L:	nT	Raw Total Magnetic field data (left sensor)
Mag1_R:	nT	Raw Total Magnetic field data (right sensor)
Basemag:	nT	Magnetic diurnal variation data
Mag2_L:	nT	Diurnal corrected Total Magnetic field data (left sensor)
Mag2_R:	nT	Diurnal corrected Total Magnetic field data (right sensor)
Mag2LZ	nT	Tilt Corrected Mag2_L (Left Sensor)
Mag2RZ	nT	Tilt Corrected Mag2_R (Right Sensor)
Mag2CZ	nT	(Mag2LZ+ Mag2RZ)/2
Mag3CZ:	nT	Levelled Mag2CZ
CVG	nT/m	Calculated Vertical Gradient of TMI
SFz[14]:	pV/(A*m ⁴)	Z dB/dt 96 microsecond time channel
SFz[15]:	pV/(A*m ⁴)	Z dB/dt 110 microsecond time channel
SFz[16]:	pV/(A*m ⁴)	Z dB/dt 126 microsecond time channel
SFz[17]:	pV/(A*m ⁴)	Z dB/dt 145 microsecond time channel
SFz[18]:	pV/(A*m ⁴)	Z dB/dt 167 microsecond time channel
SFz[19]:	pV/(A*m ⁴)	Z dB/dt 192 microsecond time channel
SFz[20]:	pV/(A*m ⁴)	Z dB/dt 220 microsecond time channel
SFz[21]:	pV/(A*m ⁴)	Z dB/dt 253 microsecond time channel
SFz[22]:	pV/(A*m ⁴)	Z dB/dt 290 microsecond time channel
SFz[23]:	pV/(A*m ⁴)	Z dB/dt 333 microsecond time channel
SFz[24]:	pV/(A*m ⁴)	Z dB/dt 383 microsecond time channel
SFz[25]:	pV/(A*m ⁴)	Z dB/dt 440 microsecond time channel
SFz[26]:	pV/(A*m ⁴)	Z dB/dt 505 microsecond time channel
SFz[27]:	pV/(A*m ⁴)	Z dB/dt 580 microsecond time channel
SFz[28]:	pV/(A*m ⁴)	Z dB/dt 667 microsecond time channel
SFz[29]:	pV/(A*m ⁴)	Z dB/dt 766 microsecond time channel
SFz[30]:	pV/(A*m ⁴)	Z dB/dt 880 microsecond time channel
SFz[31]:	pV/(A*m ⁴)	Z dB/dt 1010 microsecond time channel
SFz[32]:	pV/(A*m ⁴)	Z dB/dt 1161 microsecond time channel
SFz[33]:	pV/(A*m ⁴)	Z dB/dt 1333 microsecond time channel
SFz[34]:	pV/(A*m ⁴)	Z dB/dt 1531 microsecond time channel
SFz[35]:	pV/(A*m ⁴)	Z dB/dt 1760 microsecond time channel
SFz[36]:	pV/(A*m ⁴)	Z dB/dt 2021 microsecond time channel
SFz[37]:	pV/(A*m ⁴)	Z dB/dt 2323 microsecond time channel
SFz[38]:	pV/(A*m ⁴)	Z dB/dt 2667 microsecond time channel
SFz[39]:	pV/(A*m ⁴)	Z dB/dt 3063 microsecond time channel
SFz[40]:	pV/(A*m ⁴)	Z dB/dt 3521 microsecond time channel
SFz[41]:	pV/(A*m ⁴)	Z dB/dt 4042 microsecond time channel
SFz[42]:	pV/(A*m ⁴)	Z dB/dt 4641 microsecond time channel
SFz[43]:	pV/(A*m ⁴)	Z dB/dt 5333 microsecond time channel

Channel name	Units	Description
SFz[44]:	$\text{pV}/(\text{A}\cdot\text{m}^4)$	Z dB/dt 6125 microsecond time channel
SFz[45]:	$\text{pV}/(\text{A}\cdot\text{m}^4)$	Z dB/dt 7036 microsecond time channel
SFx[20]:	$\text{pV}/(\text{A}\cdot\text{m}^4)$	X dB/dt 220 microsecond time channel
SFx[21]:	$\text{pV}/(\text{A}\cdot\text{m}^4)$	X dB/dt 253 microsecond time channel
SFx[22]:	$\text{pV}/(\text{A}\cdot\text{m}^4)$	X dB/dt 290 microsecond time channel
SFx[23]:	$\text{pV}/(\text{A}\cdot\text{m}^4)$	X dB/dt 333 microsecond time channel
SFx[24]:	$\text{pV}/(\text{A}\cdot\text{m}^4)$	X dB/dt 383 microsecond time channel
SFx[25]:	$\text{pV}/(\text{A}\cdot\text{m}^4)$	X dB/dt 440 microsecond time channel
SFx[26]:	$\text{pV}/(\text{A}\cdot\text{m}^4)$	X dB/dt 505 microsecond time channel
SFx[27]:	$\text{pV}/(\text{A}\cdot\text{m}^4)$	X dB/dt 580 microsecond time channel
SFx[28]:	$\text{pV}/(\text{A}\cdot\text{m}^4)$	X dB/dt 667 microsecond time channel
SFx[29]:	$\text{pV}/(\text{A}\cdot\text{m}^4)$	X dB/dt 766 microsecond time channel
SFx[30]:	$\text{pV}/(\text{A}\cdot\text{m}^4)$	X dB/dt 880 microsecond time channel
SFx[31]:	$\text{pV}/(\text{A}\cdot\text{m}^4)$	X dB/dt 1010 microsecond time channel
SFx[32]:	$\text{pV}/(\text{A}\cdot\text{m}^4)$	X dB/dt 1161 microsecond time channel
SFx[33]:	$\text{pV}/(\text{A}\cdot\text{m}^4)$	X dB/dt 1333 microsecond time channel
SFx[34]:	$\text{pV}/(\text{A}\cdot\text{m}^4)$	X dB/dt 1531 microsecond time channel
SFx[35]:	$\text{pV}/(\text{A}\cdot\text{m}^4)$	X dB/dt 1760 microsecond time channel
SFx[36]:	$\text{pV}/(\text{A}\cdot\text{m}^4)$	X dB/dt 2021 microsecond time channel
SFx[37]:	$\text{pV}/(\text{A}\cdot\text{m}^4)$	X dB/dt 2323 microsecond time channel
SFx[38]:	$\text{pV}/(\text{A}\cdot\text{m}^4)$	X dB/dt 2667 microsecond time channel
SFx[39]:	$\text{pV}/(\text{A}\cdot\text{m}^4)$	X dB/dt 3063 microsecond time channel
SFx[40]:	$\text{pV}/(\text{A}\cdot\text{m}^4)$	X dB/dt 3521 microsecond time channel
SFx[41]:	$\text{pV}/(\text{A}\cdot\text{m}^4)$	X dB/dt 4042 microsecond time channel
SFx[42]:	$\text{pV}/(\text{A}\cdot\text{m}^4)$	X dB/dt 4641 microsecond time channel
SFx[43]:	$\text{pV}/(\text{A}\cdot\text{m}^4)$	X dB/dt 5333 microsecond time channel
SFx[44]:	$\text{pV}/(\text{A}\cdot\text{m}^4)$	X dB/dt 6125 microsecond time channel
SFx[45]:	$\text{pV}/(\text{A}\cdot\text{m}^4)$	X dB/dt 7036 microsecond time channel
BFz	$(\text{pV}\cdot\text{ms})/(\text{A}\cdot\text{m}^4)$	Z B-Field data for time channels 14 to 45
BFx	$(\text{pV}\cdot\text{ms})/(\text{A}\cdot\text{m}^4)$	X B-Field data for time channels 20 to 45
SFxFF	$\text{pV}/(\text{A}\cdot\text{m}^4)$	Fraser Filtered X dB/dt
Nchan_BF		Latest time channels of TAU calculation
Nchan_SF		Latest time channels of TAU calculation
Tau_BF	ms	Time constant B-Field
Tau_SF	ms	Time constant dB/dt
PLM:		60 Hz power line monitor

Electromagnetic B-field and dB/dt Z component data is found in array channel format between indexes 14 – 45, and X component data from 20 – 45, as described above.

- Database of the VTEM Waveform “11117_waveform_final.gdb” in Geosoft GDB format, containing the following channels:

Time: Sampling rate interval, 5.2083 microseconds
Rx_Volt: Output voltage of the receiver coil (Volt)
Tx_Current: Output current of the transmitter (Amp)

- Grids in Geosoft GRD format, as follows:

SFz18:	dB/dt Z Component Channel 18 (Time Gate 0.167 ms)
Bfz36:	B-Field Z Component Channel 36 (Time Gate 2.021 ms)
CVG:	Calculated Magnetic Vertical Gradient (nT/m)
DEM:	Digital Elevation Model (metres)
PLM:	Power Line Monitor (60 Hz)
Hgcxline:	Measured Cross-Line Gradient (nT/m)
Hginline:	Measured In-Line Gradient (nT/m)
SFxFF30:	Fraser Filtered dB/dt Channel 30 (Time Gate 0.880 ms)
TauBF:	B-Field Z Component, Calculated Time Constant (ms)
TauSF:	dB/dt Z Component, Calculated Time Constant (ms)
TMI:	Total Magnetic Intensity (nT)
TotHGrad:	Total Horizontal Gradient (nT/m)
TiltDrv:	Tilt derivative of TMI (radians)

A Geosoft .GRD file has a .GI metadata file associated with it, containing grid projection information. A grid cell size of 12.5 metres was used.

- Maps at 1:10,000 in Geosoft MAP format, as follows:

11117_10k_**_dBdtZ:	dB/dt profiles Z Component, Time Gates 0.126 – 4.042 ms in linear – logarithmic scale.
11117_10k_**_BfieldZ:	B-field profiles Z Component, Time Gates 0.220 – 7.036 ms in linear – logarithmic scale.
11117_10k_**_SfZ18:	dB/dt early time Z Component Channel 18, Time Gate 0.167 ms colour image.
11117_10k_**_TMI:	Total Magnetic Intensity (TMI) colour image and contours.
11117_10k_**_TauSF:	dB/dt Calculated Time Constant (Tau) with contours of anomaly areas of the Calculated Vertical Derivative of TMI
11117_10k_**_TotHGrad:	Total Horizontal Gradient of Total Magnetic Intensity (TMI) colour image.
11117_10k_**_TiltDrv:	Tilt Derivative of TMI colour image.

Where ** represents block name i.e. (11117_10k_North_TMI)

Maps are also presented in PDF format.

1:50,000 topographic vectors were taken from the NRCAN Geogratis database at: <http://geogratis.gc.ca/geogratis/en/index.html>.

- A Google Earth file *11117_Flightpath.kmz* showing the flight path of the block is included. Free versions of Google Earth software from: <http://earth.google.com/download-earth.html>

6. CONCLUSIONS AND RECOMMENDATIONS

6.1 Conclusions

A helicopter-borne versatile time domain electromagnetic (VTEM) geophysical survey has been completed over the three blocks near Sudbury, Ontario.

The total area coverage is 50 km². Total survey line coverage is 1016.2 line kilometres. The principal sensors included a Time Domain EM system and a magnetic gradiometer. Results have been presented as stacked profiles, and contour color images at a scale of 1:10,000. No formal Interpretation has been included.

6.2 Recommendations

Based on the geophysical results obtained, a number of shallow and weak TEM anomalies were identified across the properties. They correspond to weak-moderate conductive targets near surface, i.e. overburden or lake sediments. No significant and strong conductors were detected. The magnetic data show numerous NW-SE trending dykes in the Ermatinger South property. In the Ermatinger North property, the main magnetic features trend SW-NE and NW-SE. There is a very strong and circular magnetic anomaly in the northern end of the Ermatinger South (B) property. We recommend a detailed interpretation of the available geophysical data, identifying magnetic lineaments, contacts, anomalous zones, possibly 2D/3D magnetic modeling and resistivity depth imaging prior to ground follow up and drill testing.

Respectfully submitted⁶,



Neil Fiset
Geotech Ltd.

Alexander Prikhodko, P. Geo
Geotech Ltd.

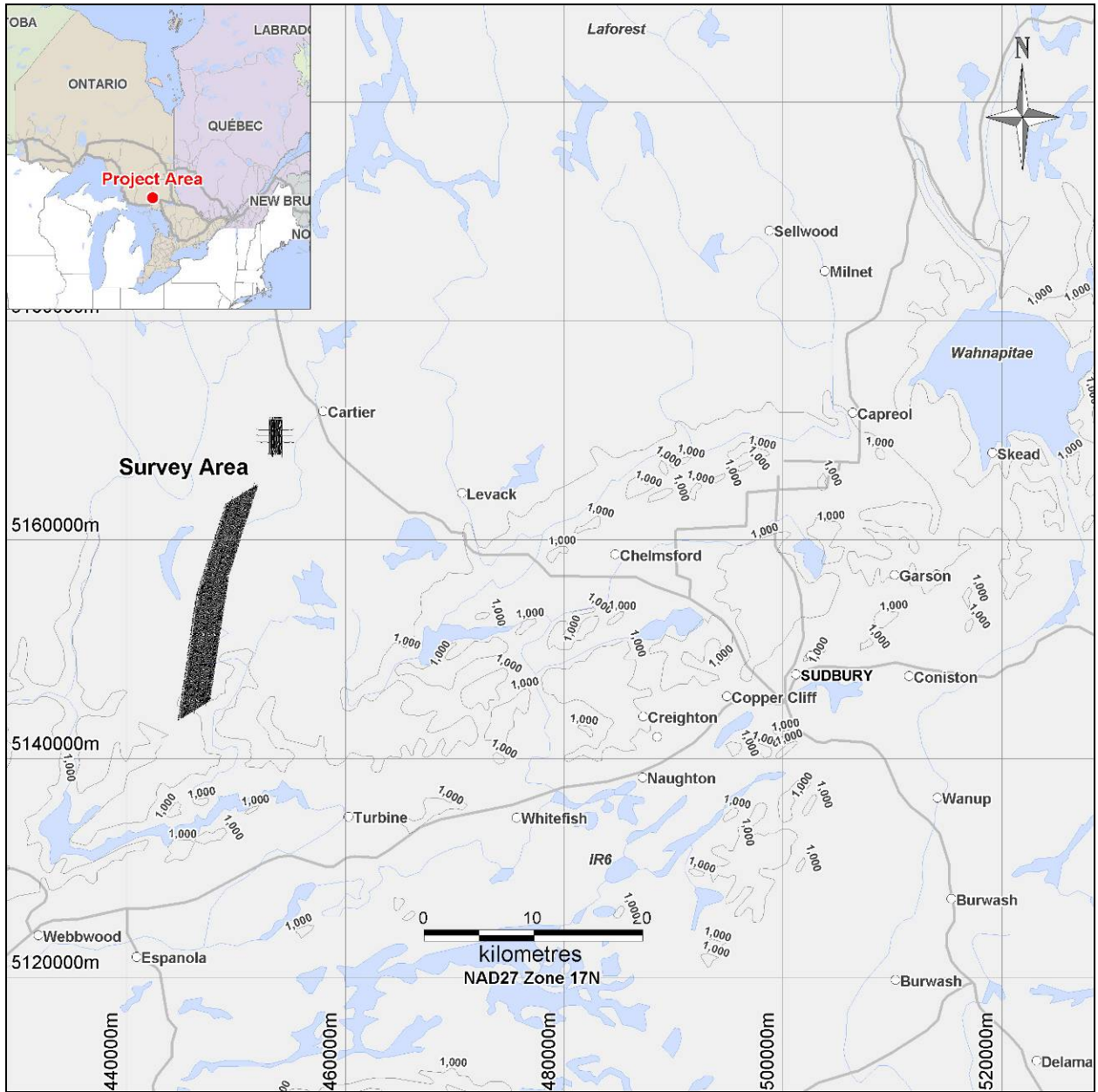
Karl Kwan
Geotech Ltd.

July, 2011

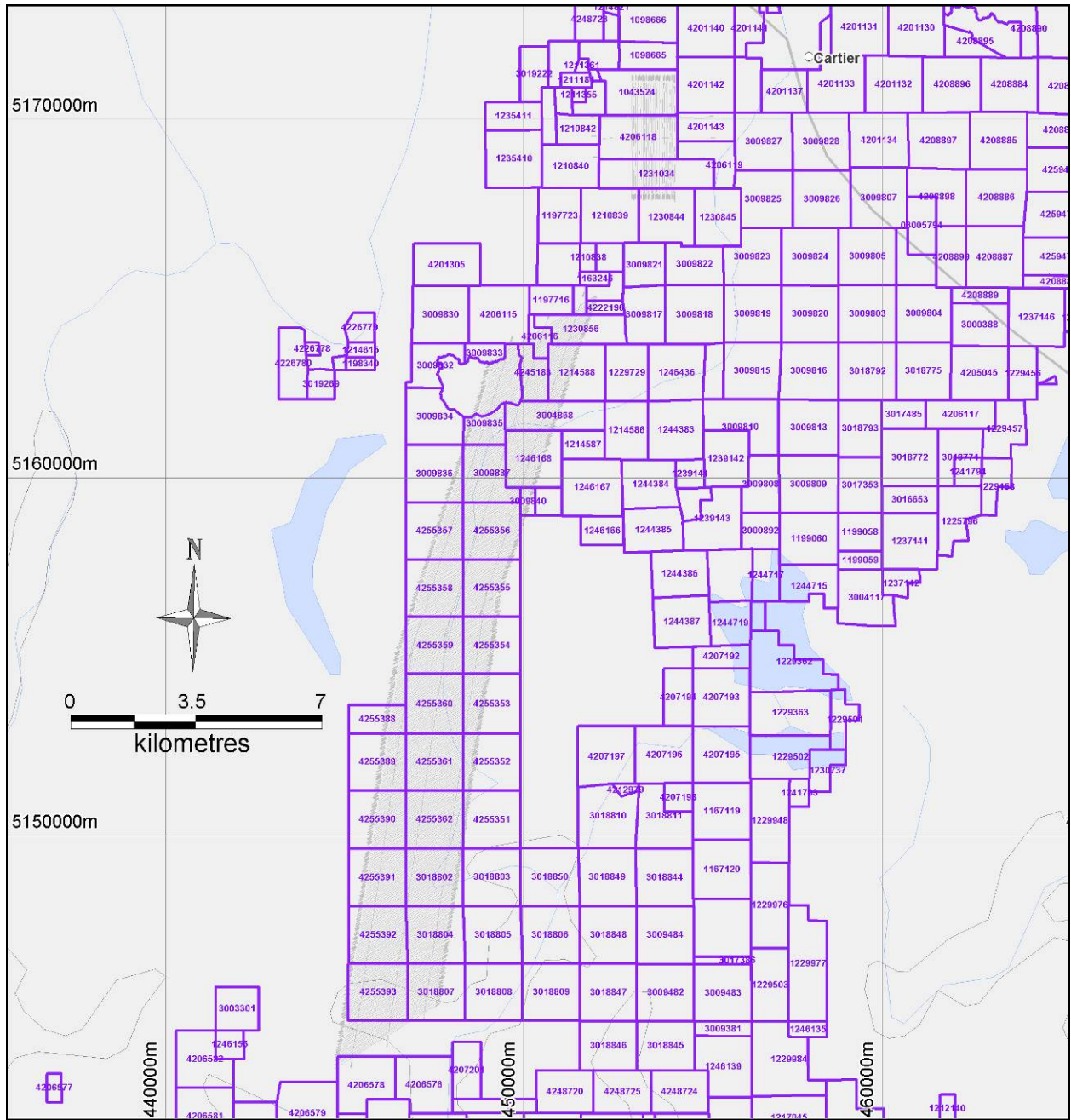
⁶Final data processing of the EM and magnetic data were carried out by Karl Kwan, from the office of Geotech Ltd. in Aurora, Ontario, under the supervision of Alexander Prikhodko, P.Geo., PhD, Senior Geophysicist, VTEM Interpretation Supervisor.

APPENDIX A

SURVEY BLOCK LOCATION MAP



Survey Overview of the Block



Flight path over Mining Claims

APPENDIX B

SURVEY BLOCK COORDINATES

(NAD 27, UTM Zone 17 North)

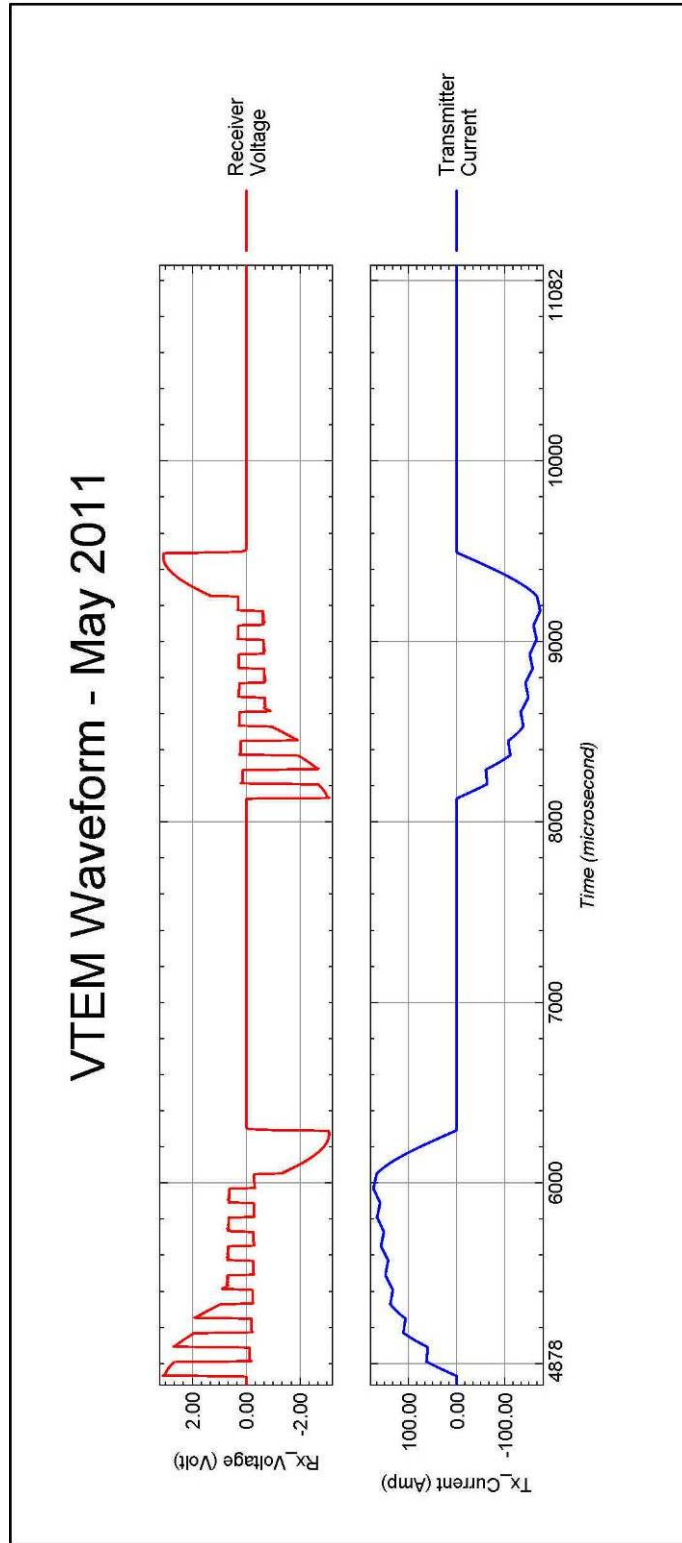
Ermatinger North	
X	Y
453021.23	5171042.25
453016.91	5167943.82
454212.87	5167939.11
454205.01	5171044.88

Ermatinger South (A)	
X	Y
449214.61	5156617.32
449005.24	5156546.74
446530.67	5155000.91
444879.88	5143600.29
447512.99	5145230.63

Ermatinger South (B)	
X	Y
446588.43	5155106.04
449285.82	5156782.65
451899.28	5164947.86
451863.93	5164983.93
449179.4	5163316.78

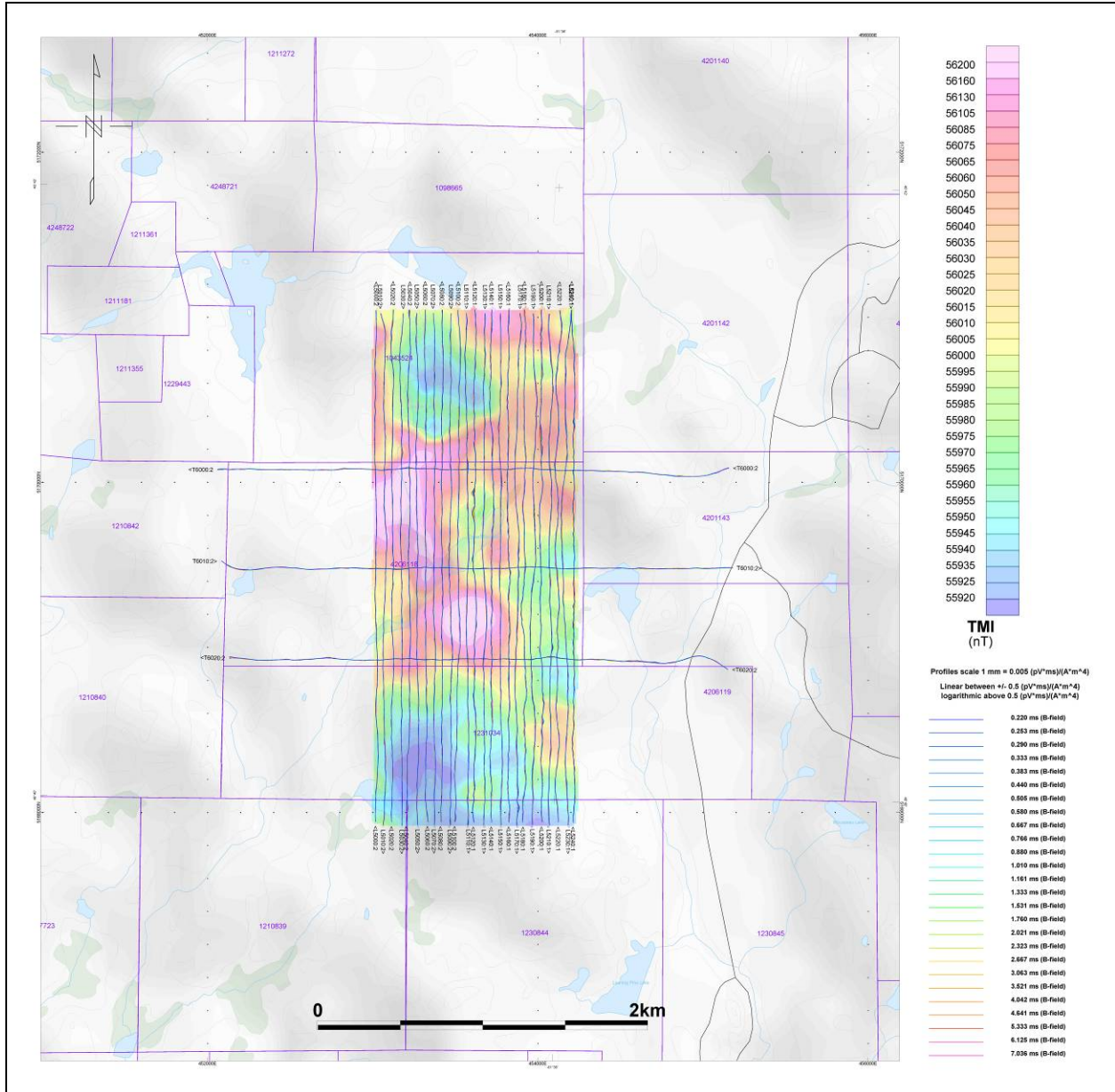
APPENDIX C

VTEM WAVEFORM



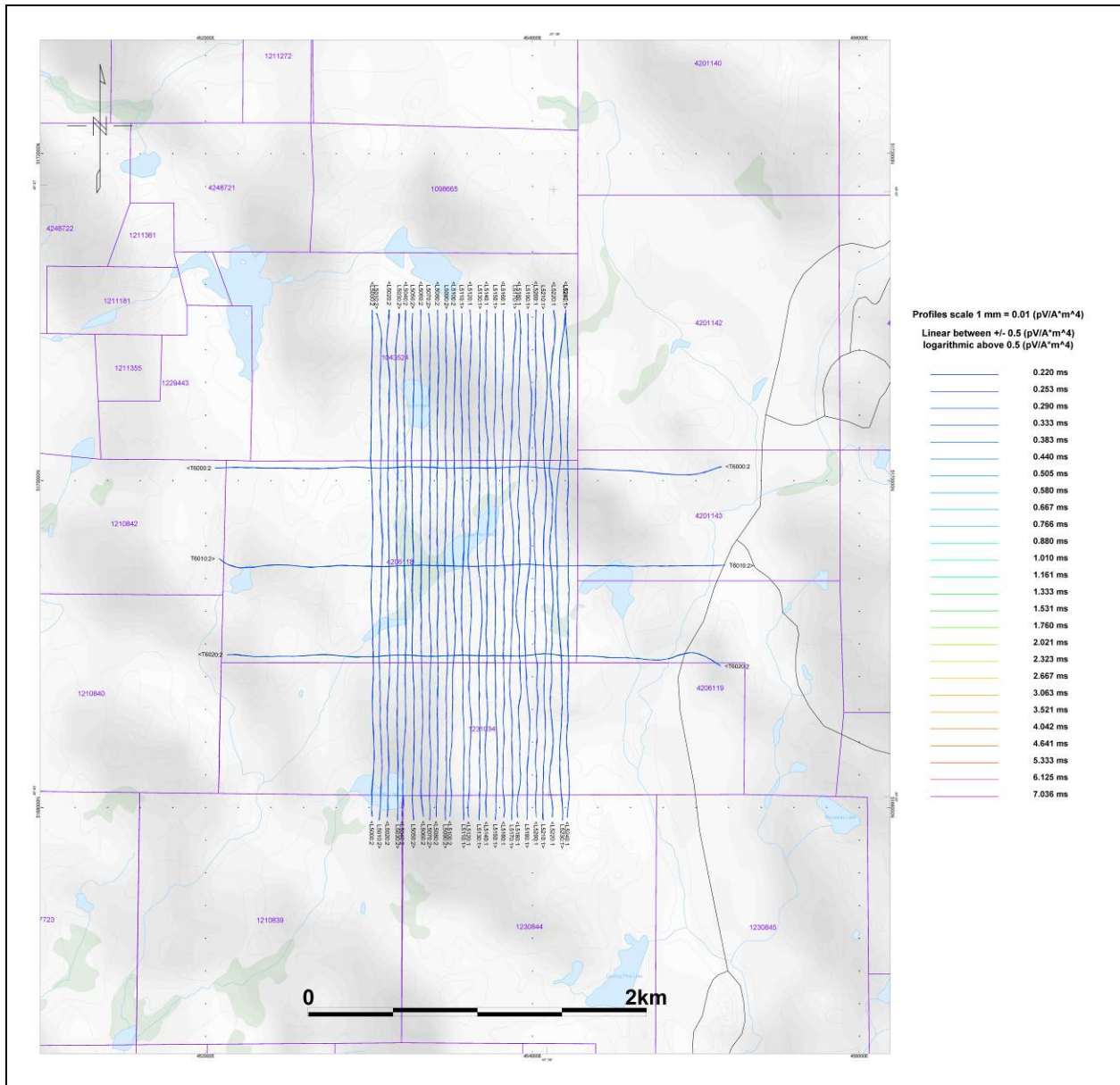
APPENDIX D

GEOPHYSICAL MAPS¹

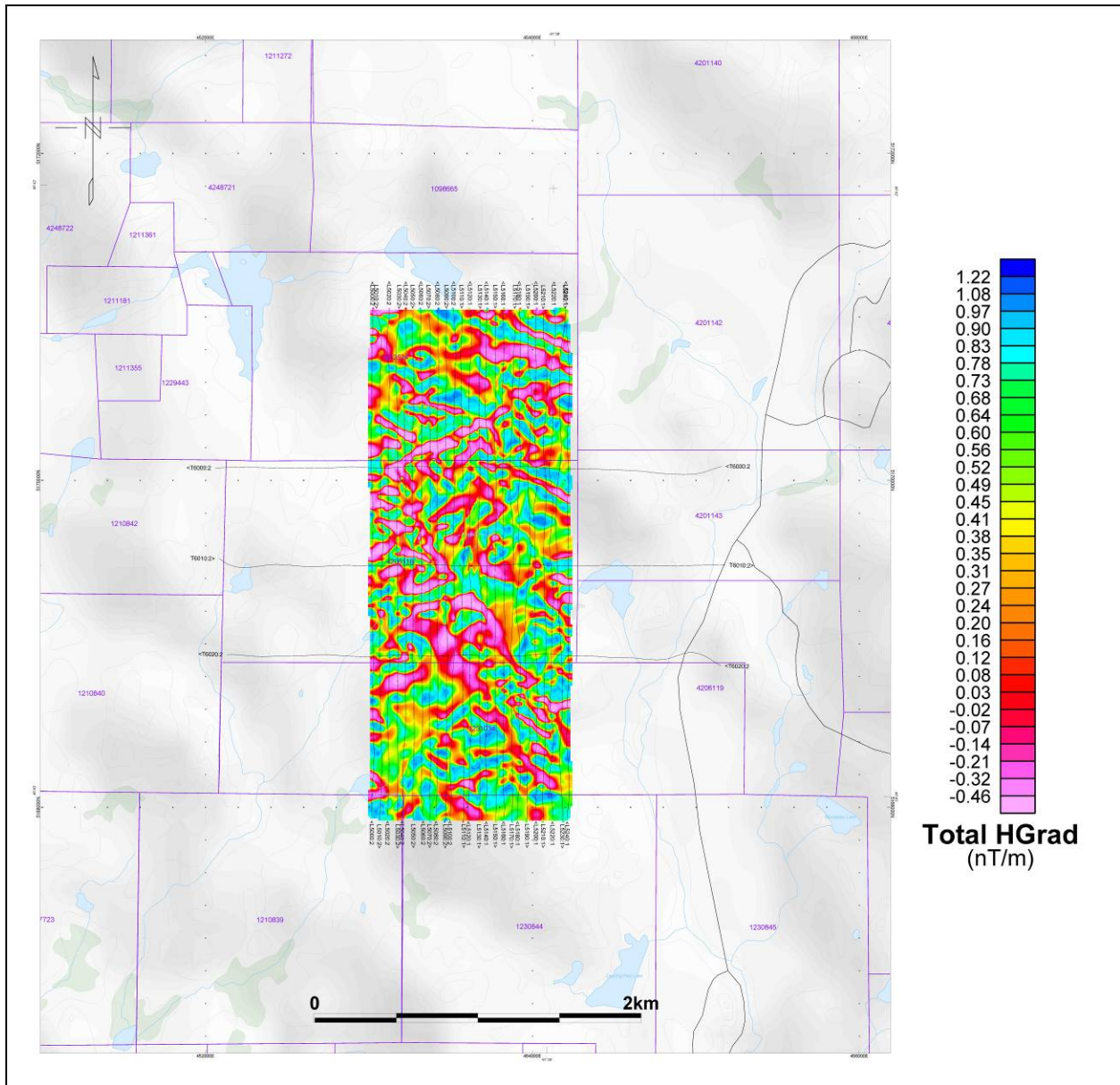


Ermatinger North - VTEM B-Field Z Component Profiles, Time Gates 0.220 to 7.036 ms

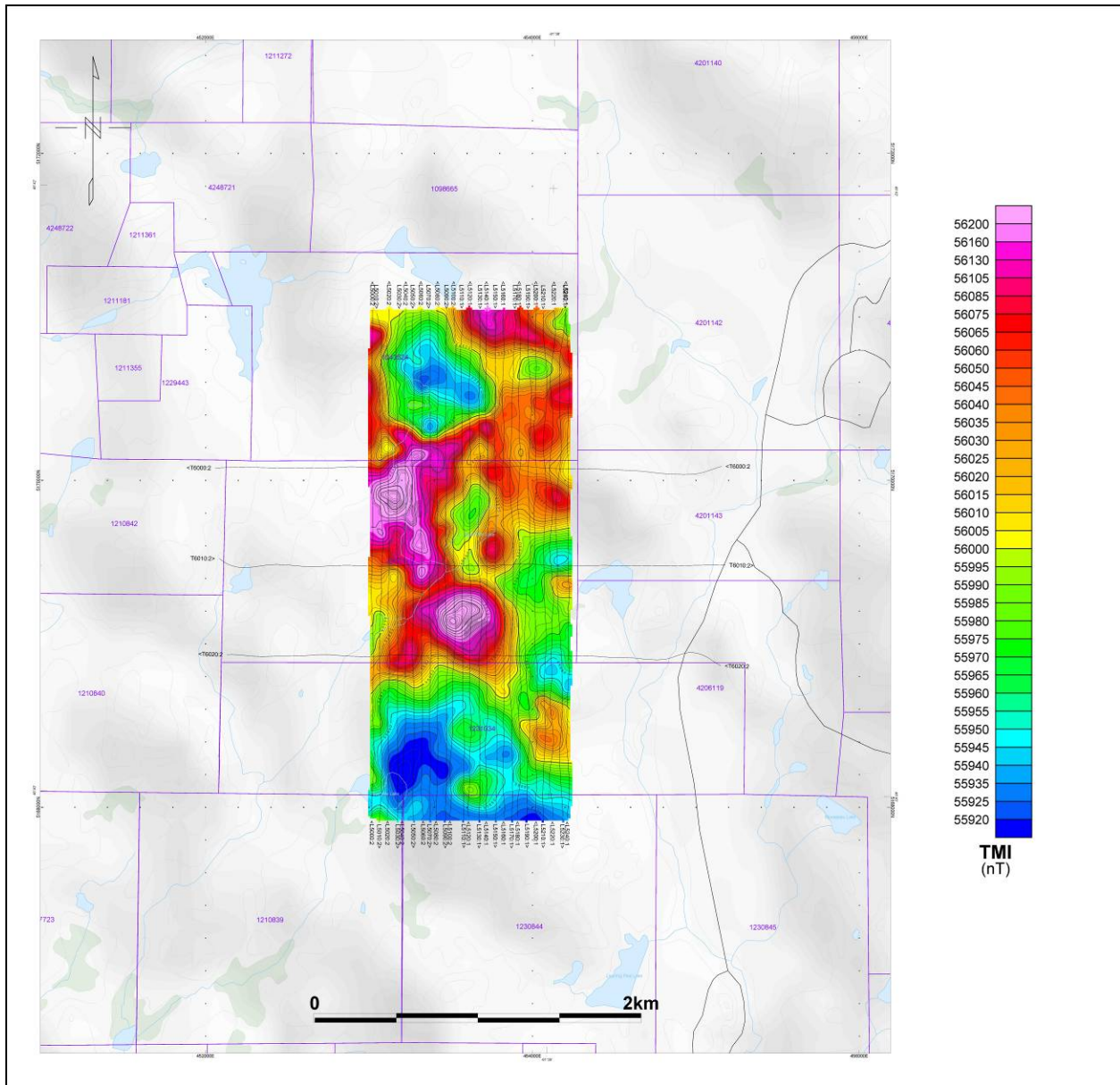
¹ Full size geophysical maps are also available in PDF format on the final DVD



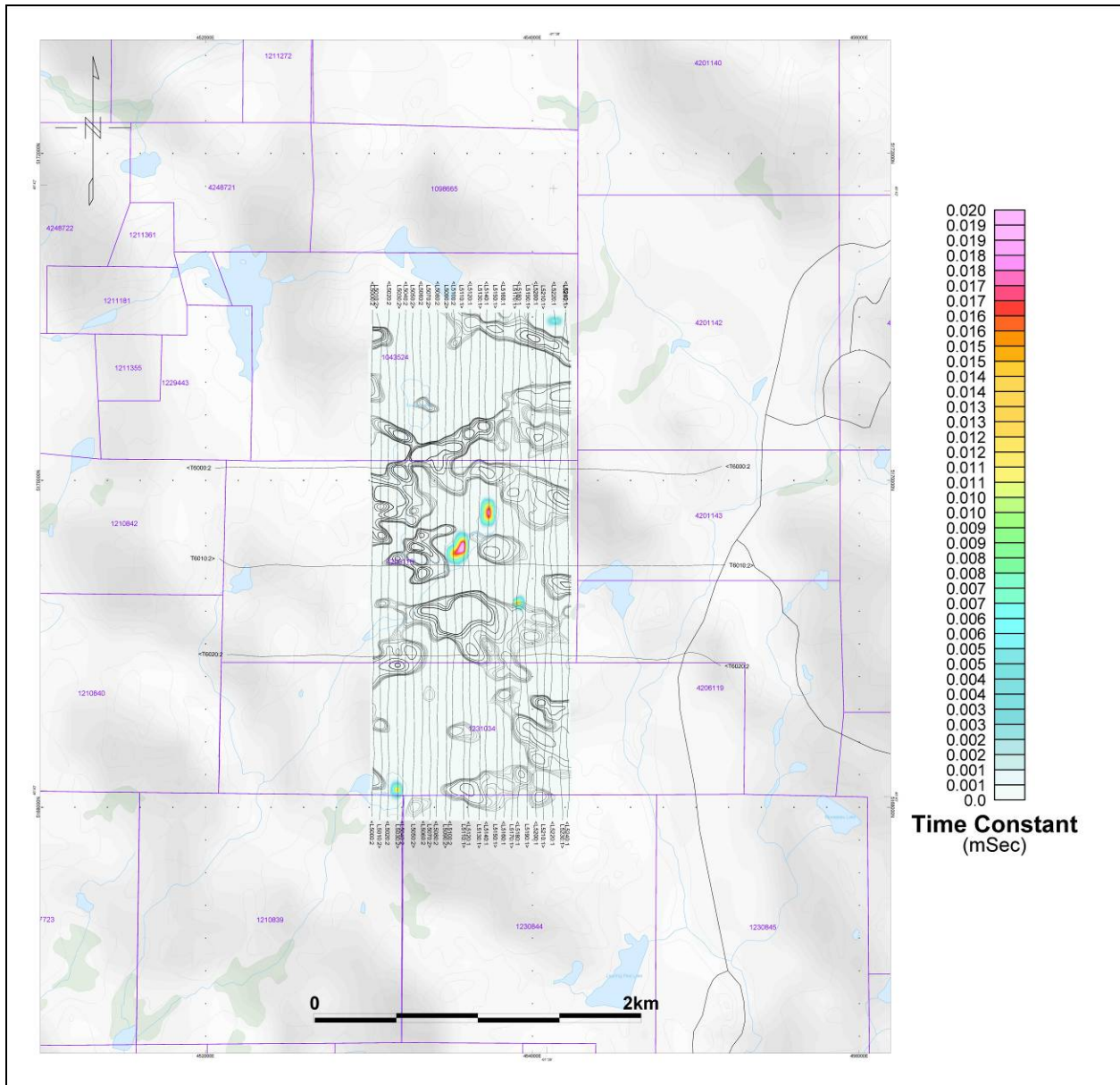
Ermatinger North - VTEM dB/dt Z Component Profiles, Time Gates 0.126 to 4.042 ms



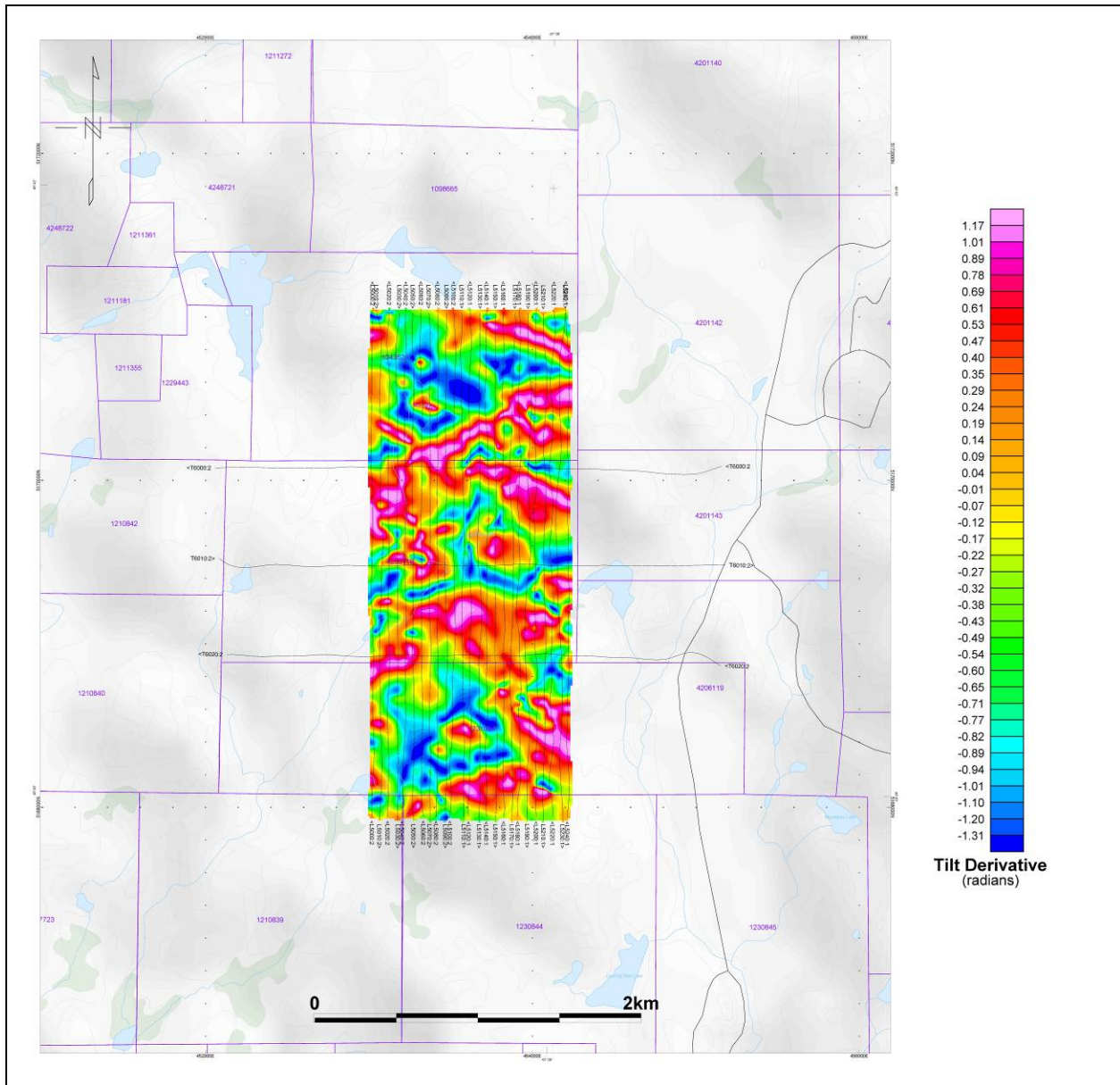
Ermatinger North - Total Horizontal Gradient of Total Magnetic Intensity



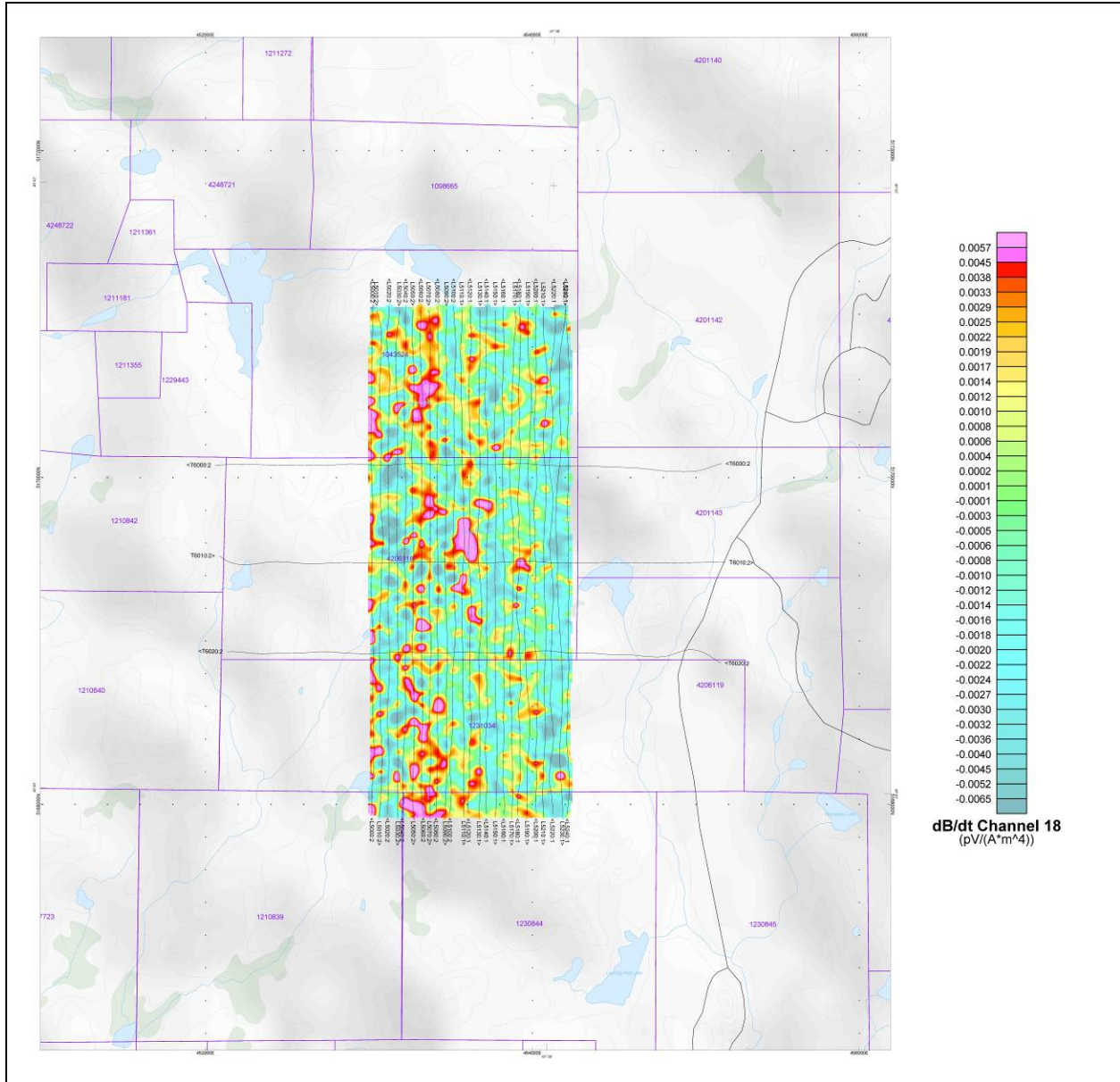
Ermatinger North - Total Magnetic Intensity (TMI)



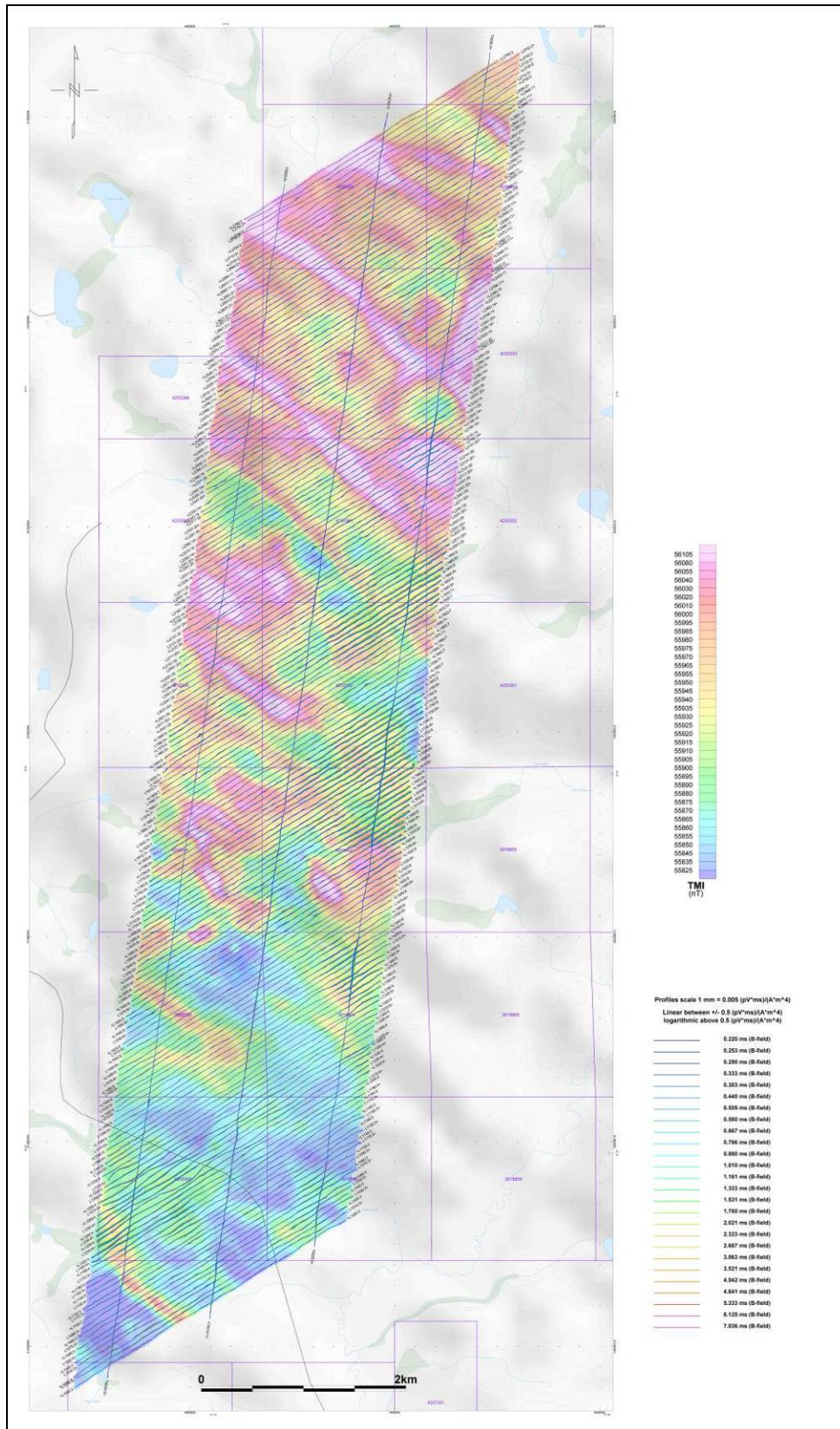
Ermatinger North - dB/dt Calculated Time Constant (Tau) with CVG contours



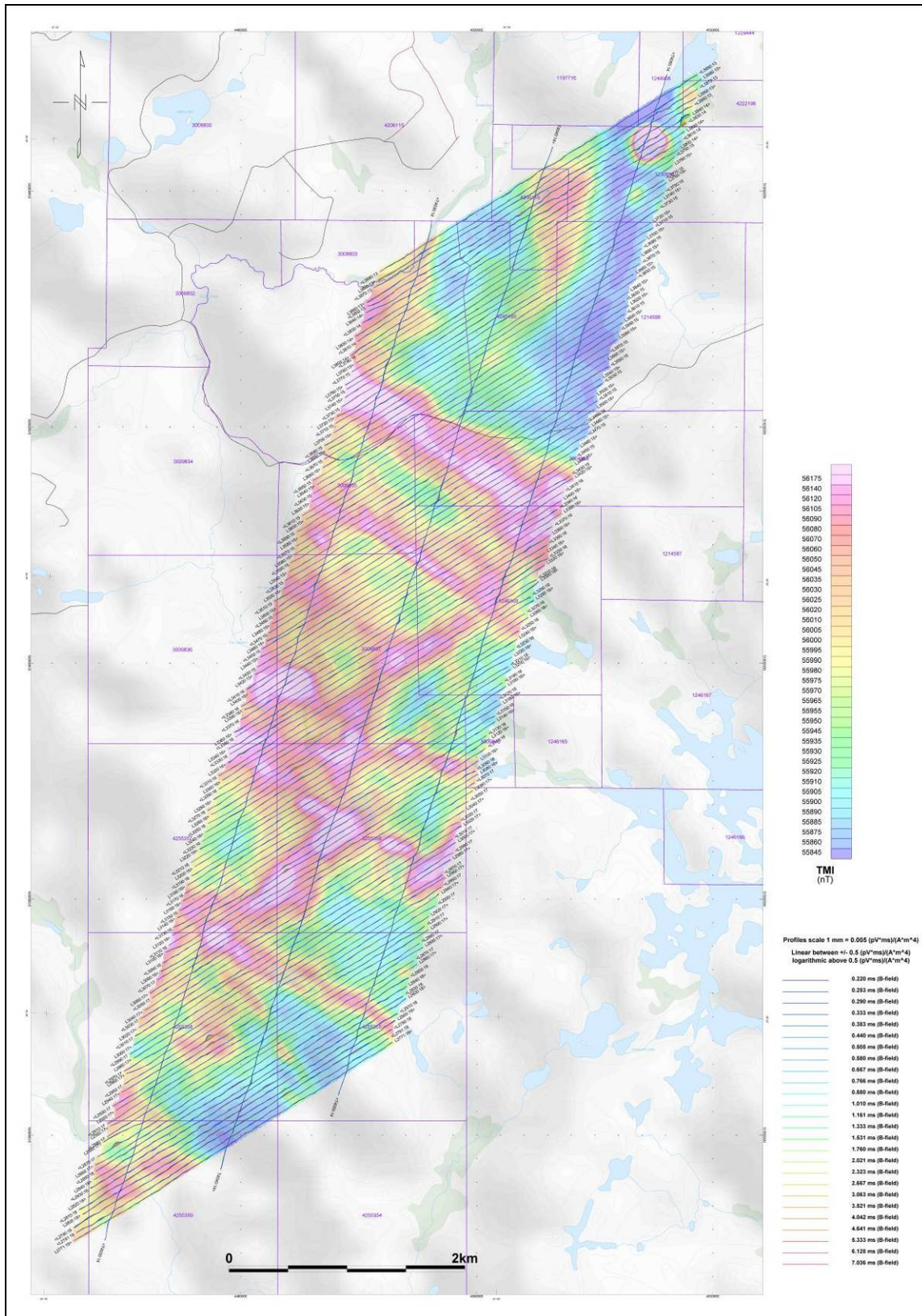
Ermatinger North - Tilt Derivative of TMI



Ermatinger North – dBdt Z Component Channel 18, Times Gate 0.167 ms



Ermatinger South(A) - VTEM B-Field Z Component Profiles, Time Gates 0.220 to 7.036 ms

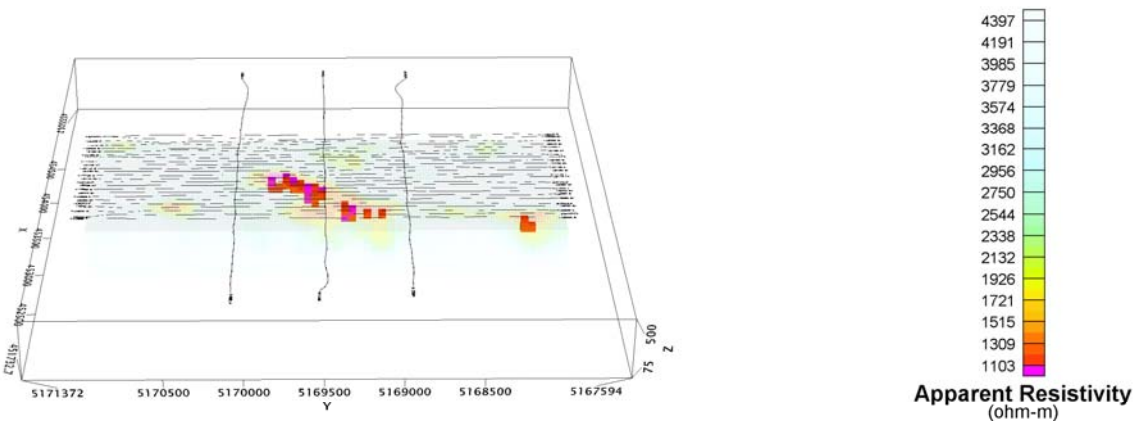
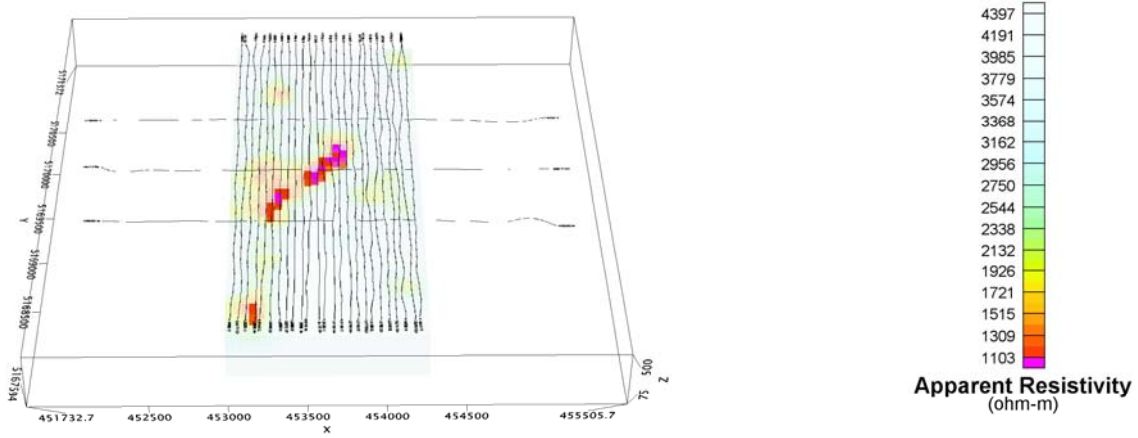


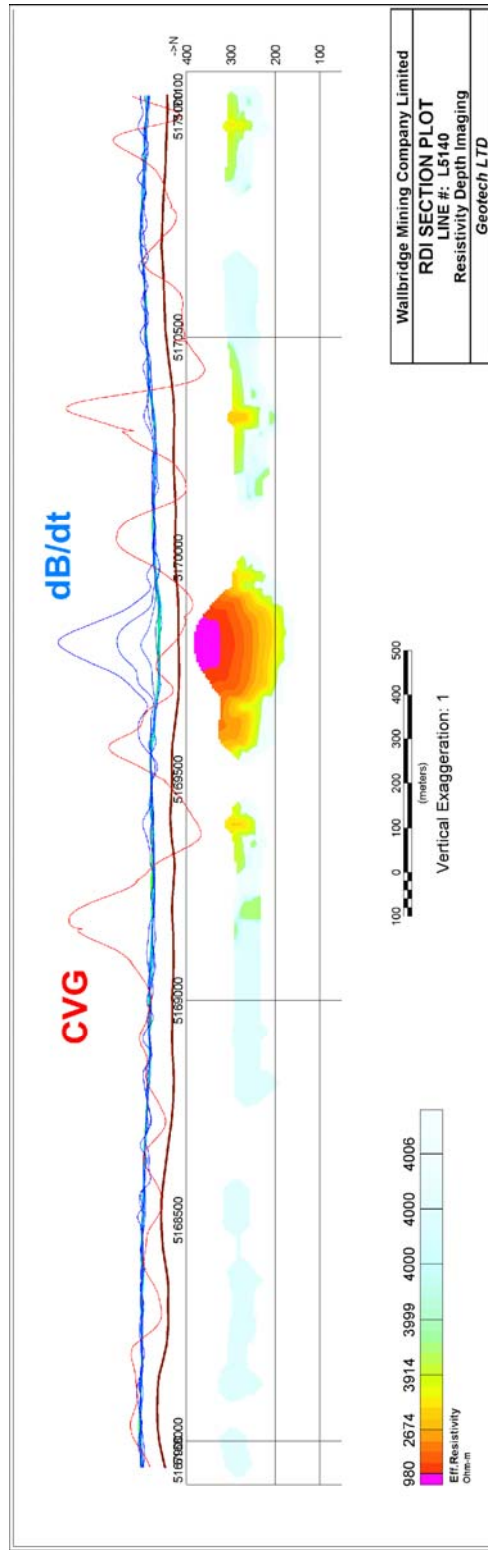
Ermatinger South(B) - VTEM B-Field Z Component Profiles, Time Gates 0.220 to 7.036 ms

Resistivity Depth Image (RDI) MAPS

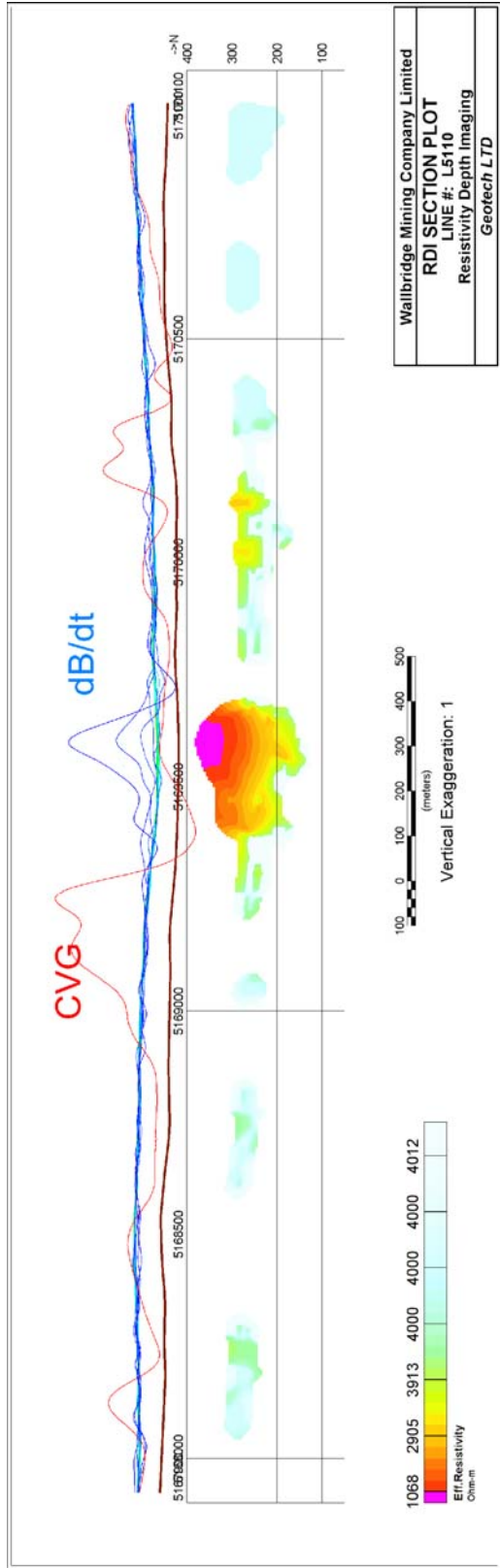
3D Resistivity-Depth Images (RDI)

Ermatinger North

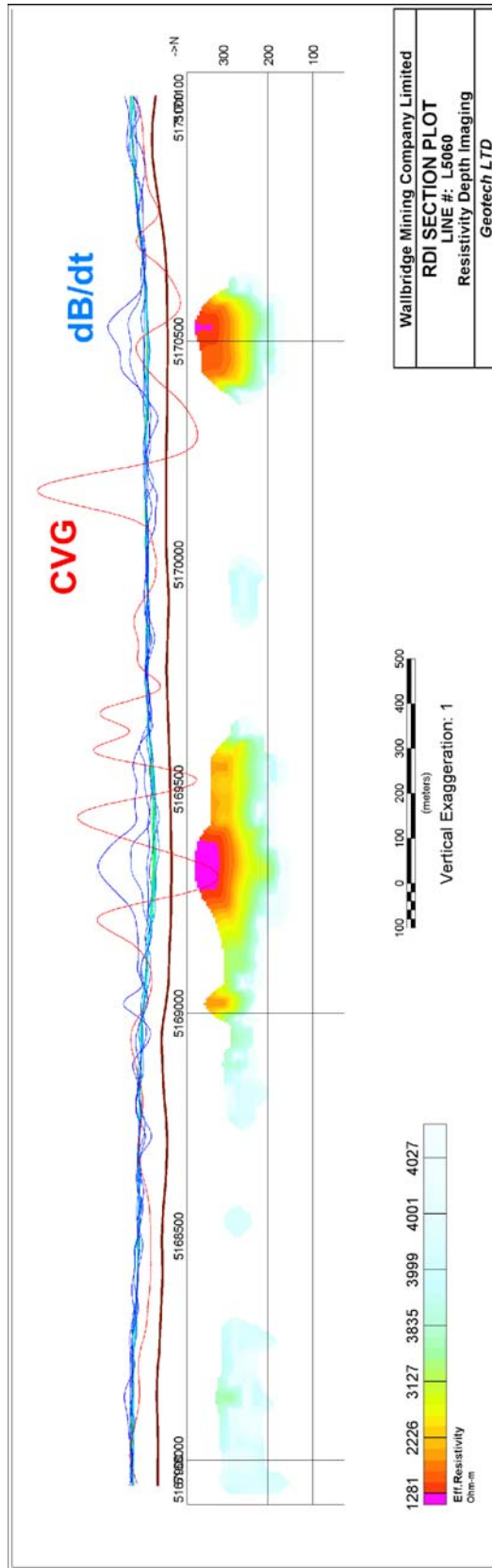




Line 5140



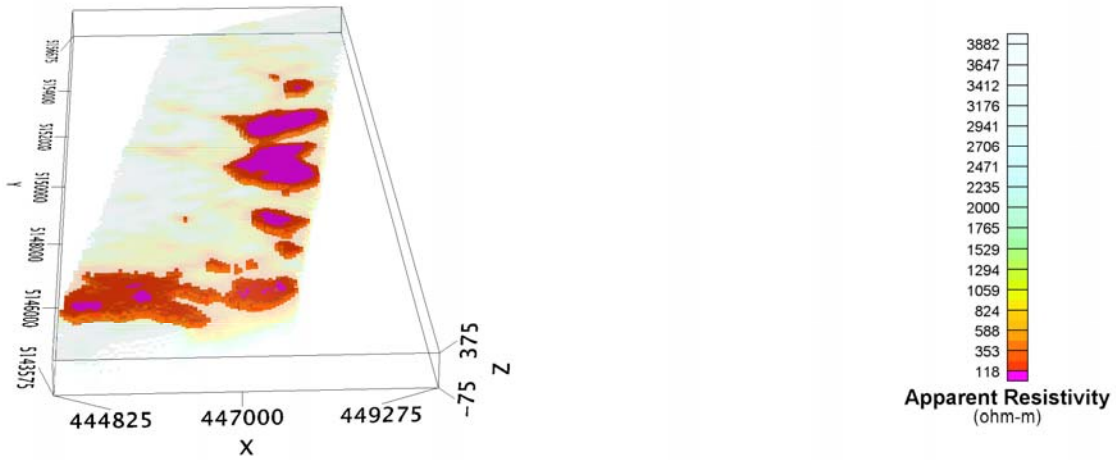
Wallbridge Mining Company Limited
RDI SECTION PLOT
 LINE #: L5110
 Resistivity Depth Imaging
 Geotech LTD



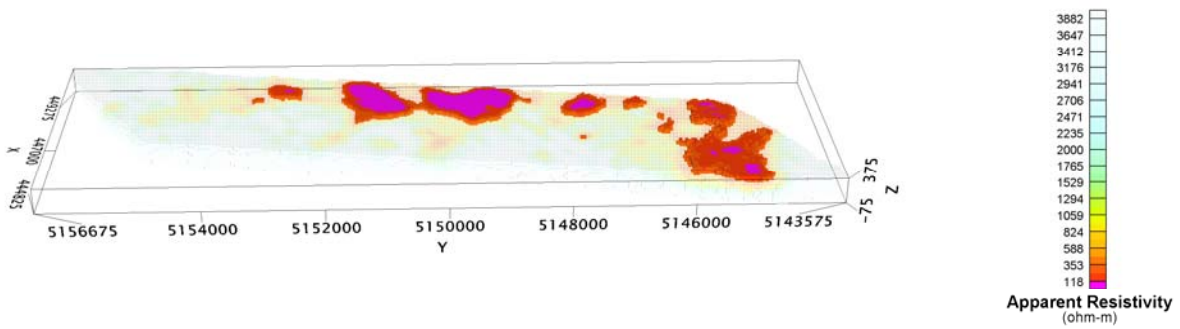
Line 5060

Wallbridge Mining Company Limited
RDI SECTION PLOT
LINE #: L5060
Resistivity Depth Imaging
Geotech LTD

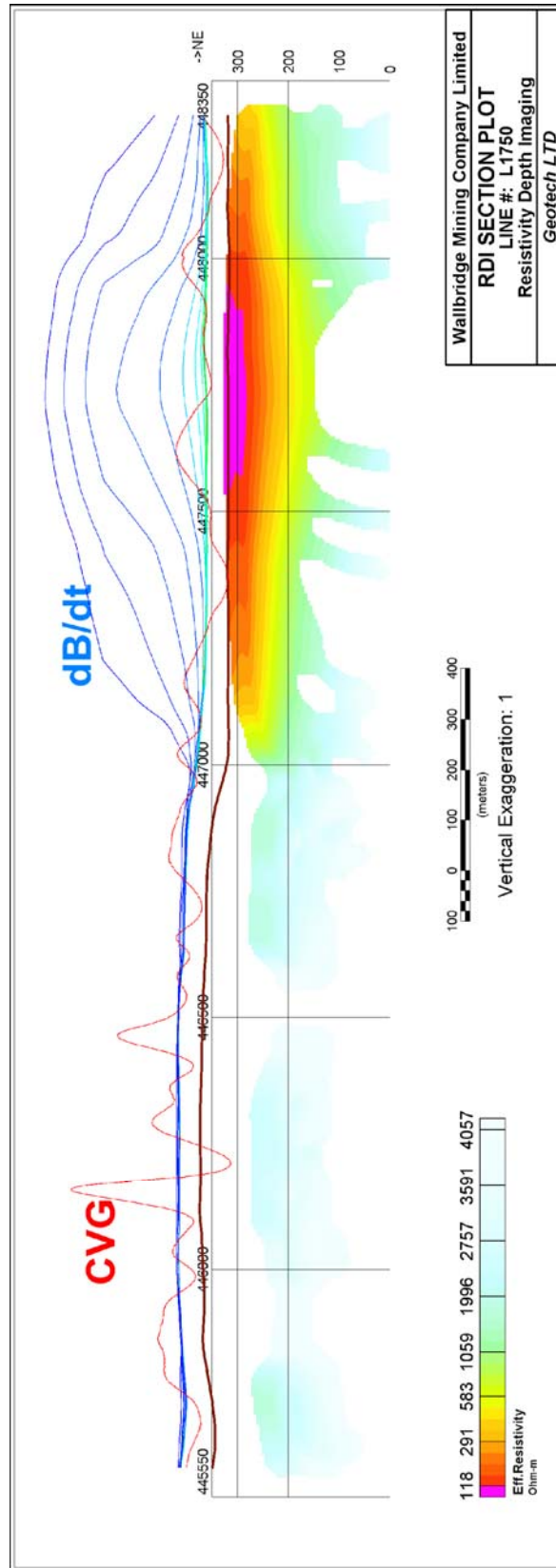
Ermatinger South (A)



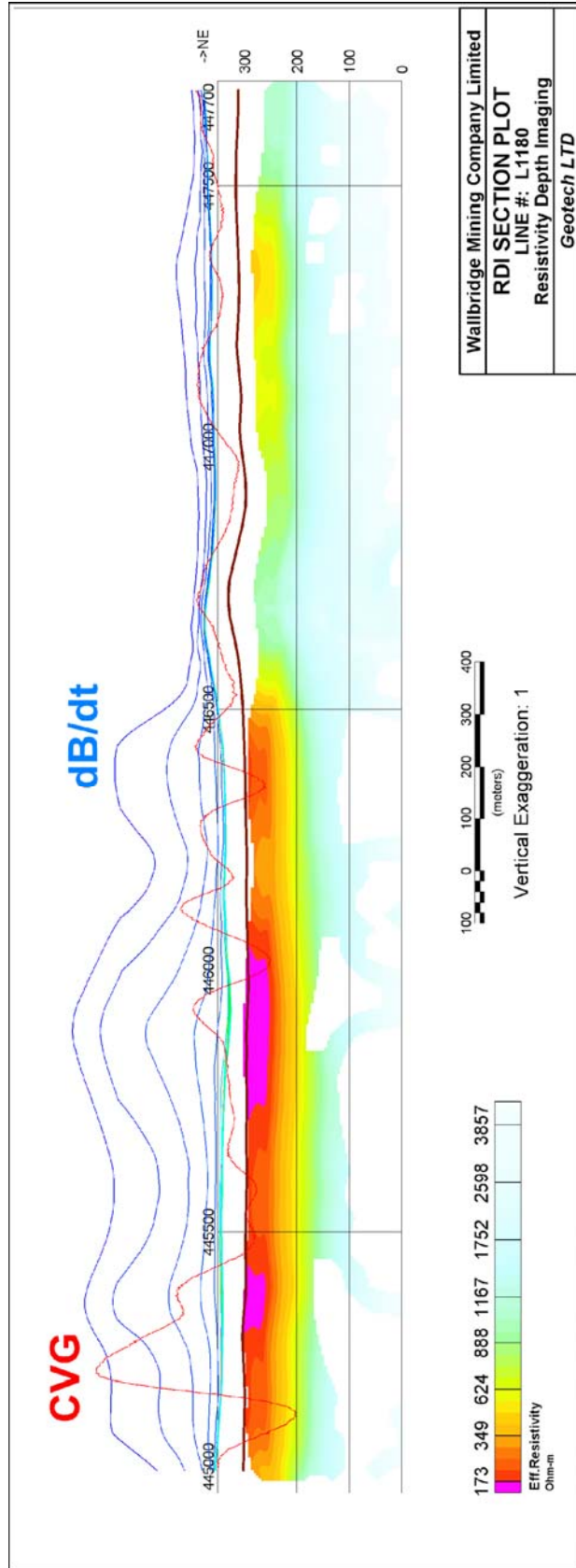
View Looking North



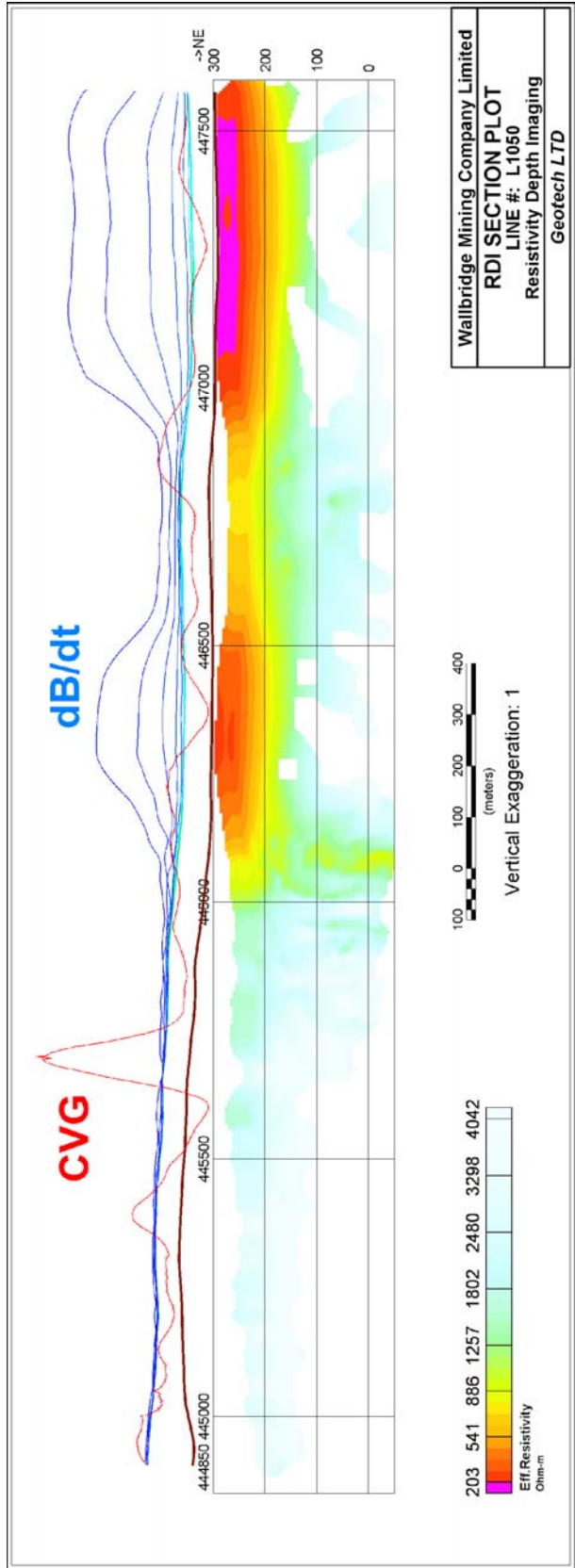
View Looking East



Line 1750



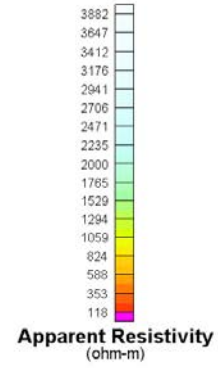
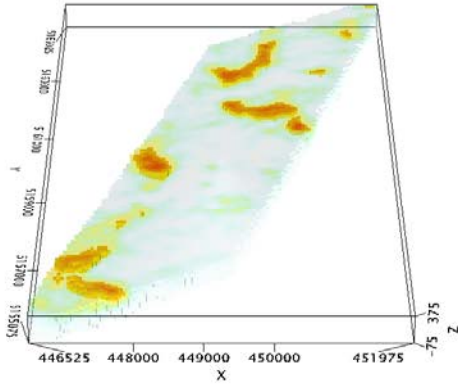
Line 1180



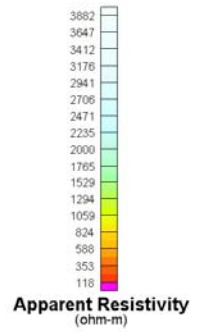
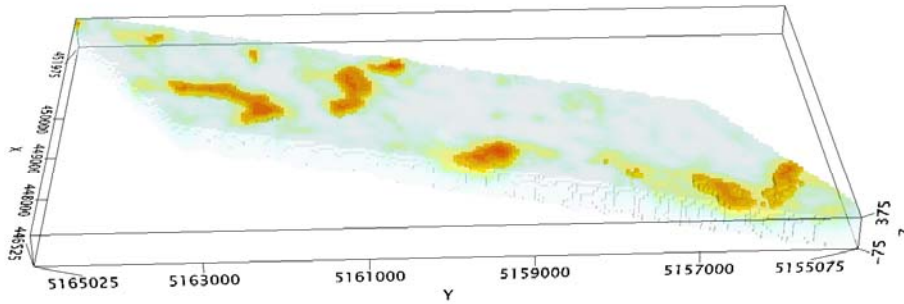
Wallbridge Mining Company Limited
RDI SECTION PLOT
 LINE #: L1050
 Resistivity Depth Imaging
 Geotech LTD

Line 1050

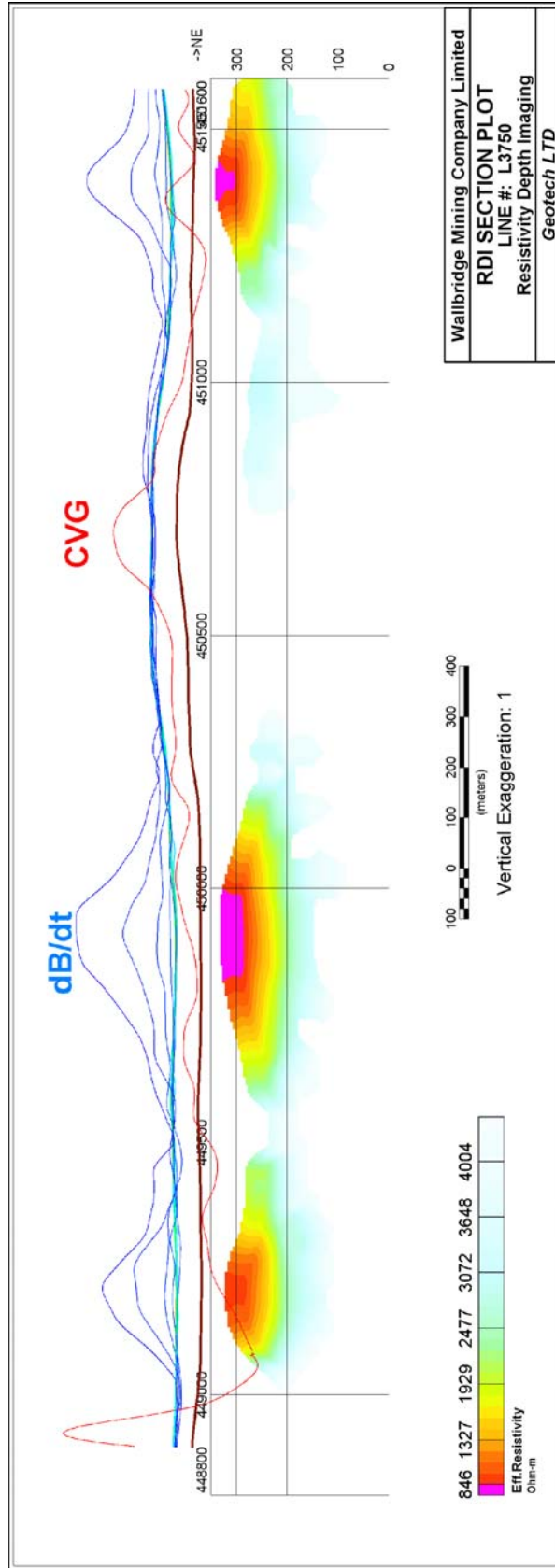
Ermatinger South (B)



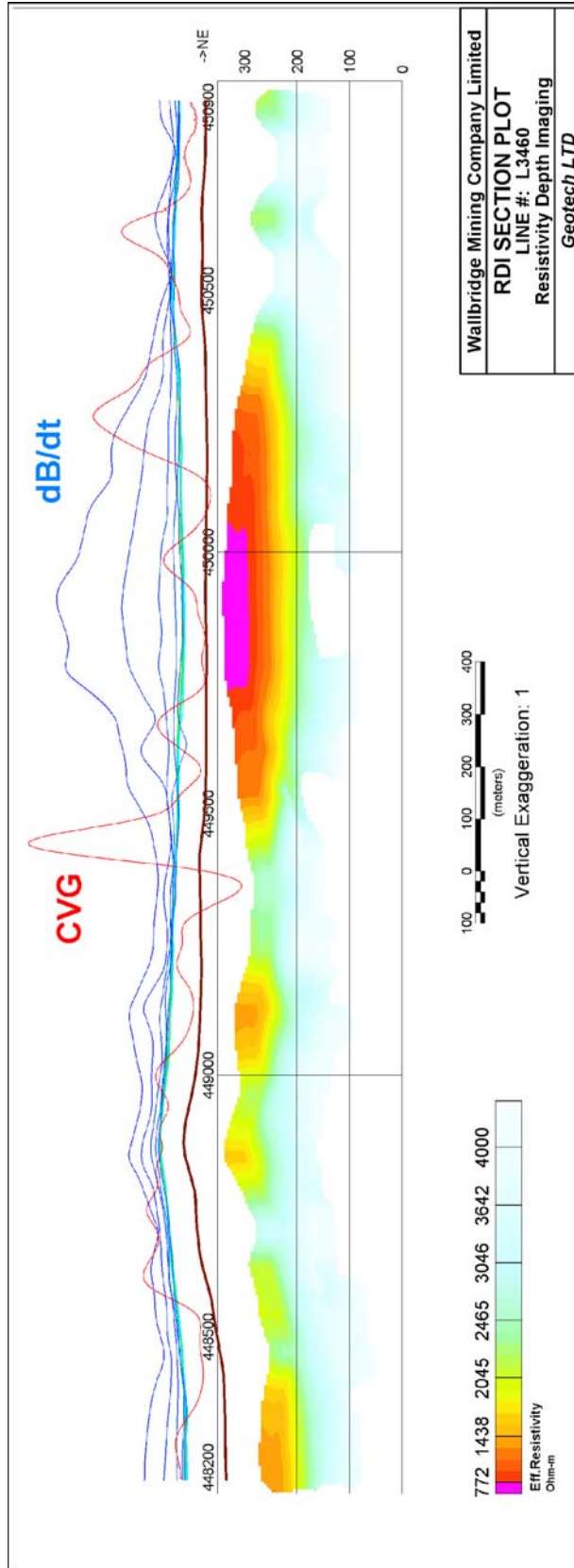
View Looking North

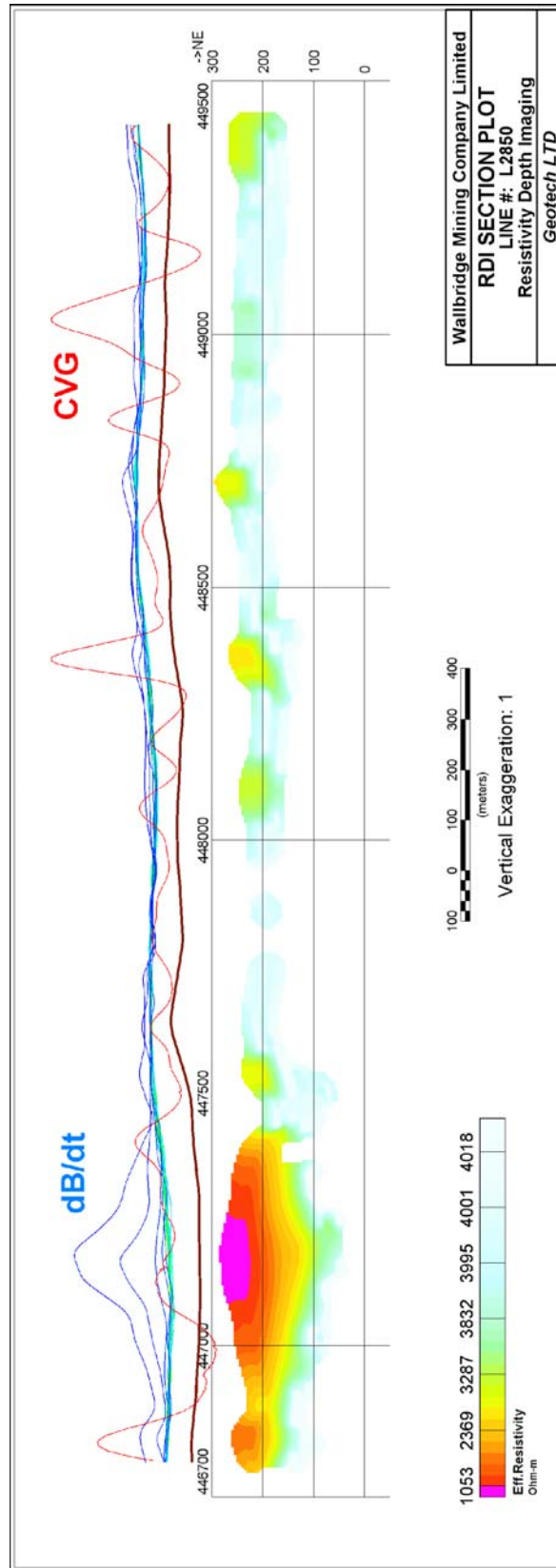


View Looking East



Line 3750





Line 2850

APPENDIX E

GENERALIZED MODELING RESULTS OF THE VTEM SYSTEM

Introduction

The VTEM system is based on a concentric or central loop design, whereby, the receiver is positioned at the centre of a transmitter loop that produces a primary field. The wave form is a bi-polar, modified square wave with a turn-on and turn-off at each end.

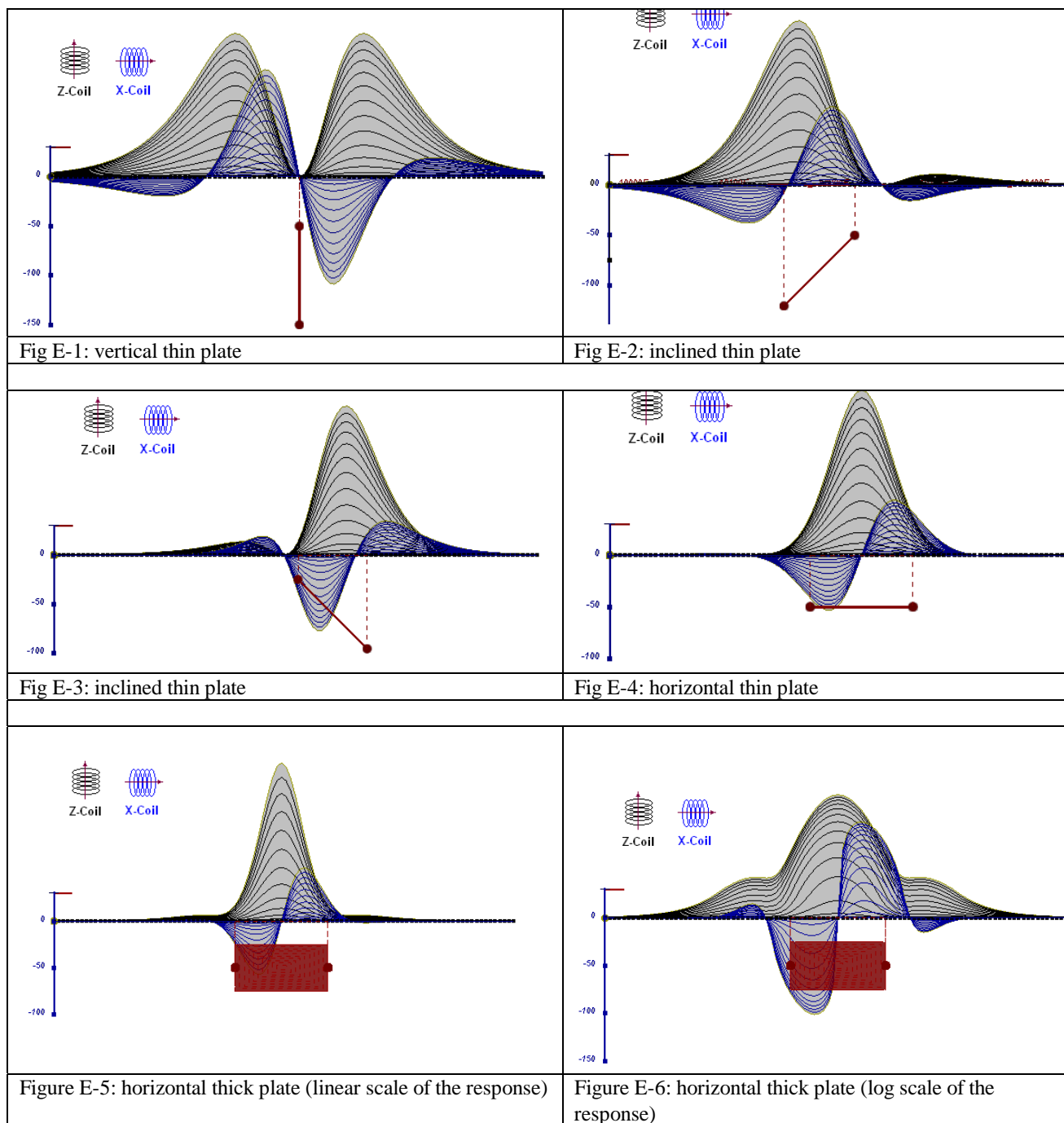
During turn-on and turn-off, a time varying field is produced (dB/dt) and an electro-motive force (emf) is created as a finite impulse response. A current ring around the transmitter loop moves outward and downward as time progresses. When conductive rocks and mineralization are encountered, a secondary field is created by mutual induction and measured by the receiver at the centre of the transmitter loop.

Efficient modeling of the results can be carried out on regularly shaped geometries, thus yielding close approximations to the parameters of the measured targets. The following is a description of a series of common models made for the purpose of promoting a general understanding of the measured results.

A set of models has been produced for the Geotech VTEM® system dB/dT Z and X components (see models E1 to E15). The Maxwell™ modeling program (EMIT Technology Pty. Ltd. Midland, WA, AU) used to generate the following responses assumes a resistive half-space. The reader is encouraged to review these models, so as to get a general understanding of the responses as they apply to survey results. While these models do not begin to cover all possibilities, they give a general perspective on the simple and most commonly encountered anomalies.

As the plate dips and departs from the vertical position, the peaks become asymmetrical.

As the dip increases, the aspect ratio (Min/Max) decreases and this aspect ratio can be used as an empirical guide to dip angles from near 90° to about 30°. The method is not sensitive enough where dips are less than about 30°.



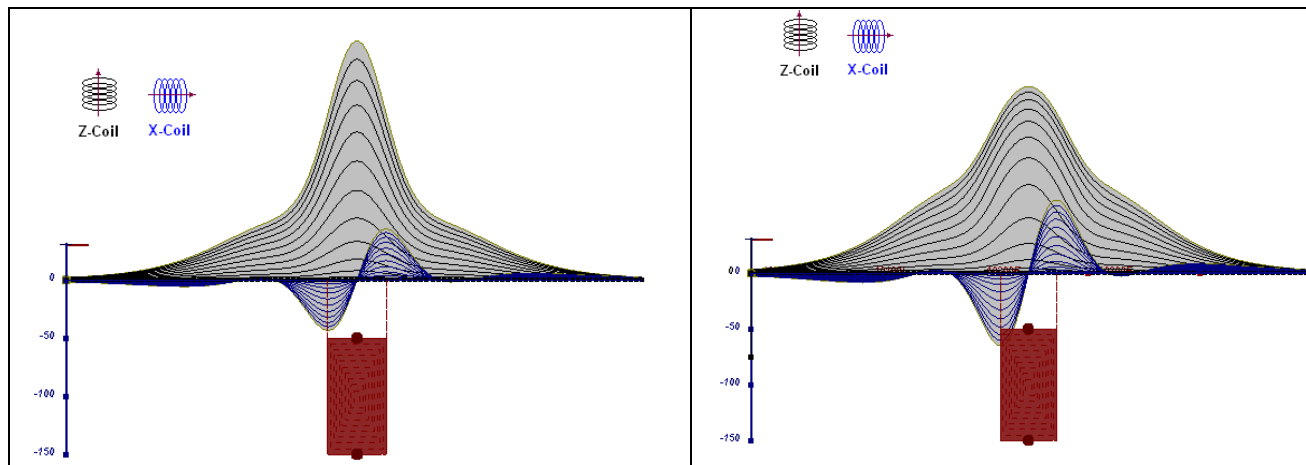


Figure E-7: vertical thick plate (linear scale of the response). 50 m depth

Figure E-8: vertical thick plate (log scale of the response). 50 m depth

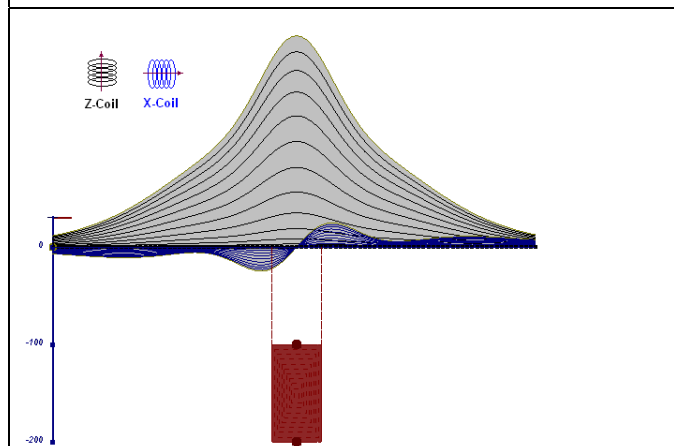


Fig E-9: vertical thick plate (linear scale of the response). 100 m depth

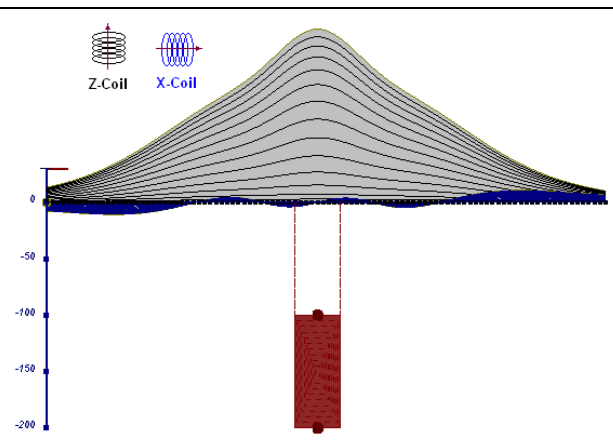


Fig E-10: vertical thick plate (linear scale of the response). Depth/hor.thickness=2.5

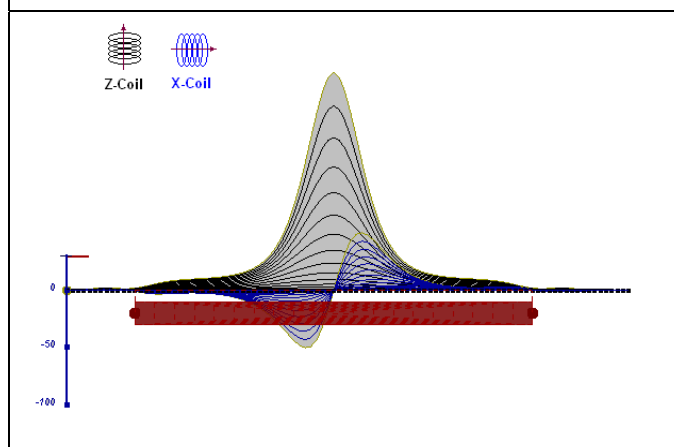


Figure E-10: horizontal thick plate (linear scale of the response)

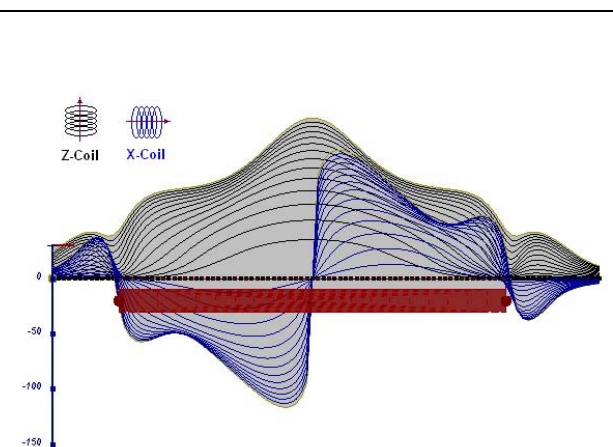


Figure E-11: horizontal thick plate (log scale of the response)

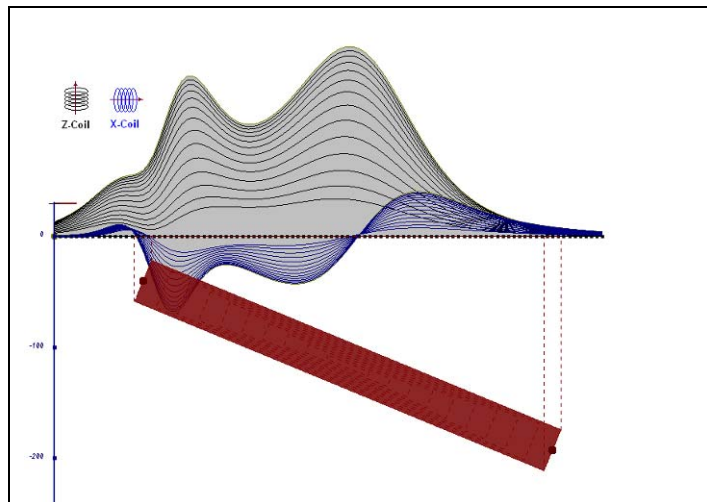


Fig E-12: inclined long thick plate

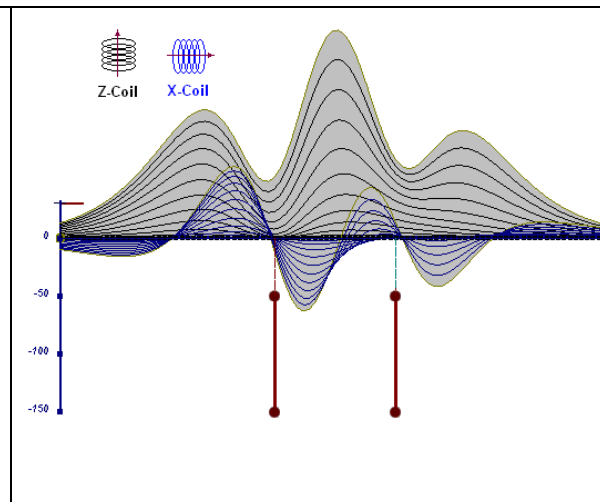


Fig E-13: two vertical thin plates

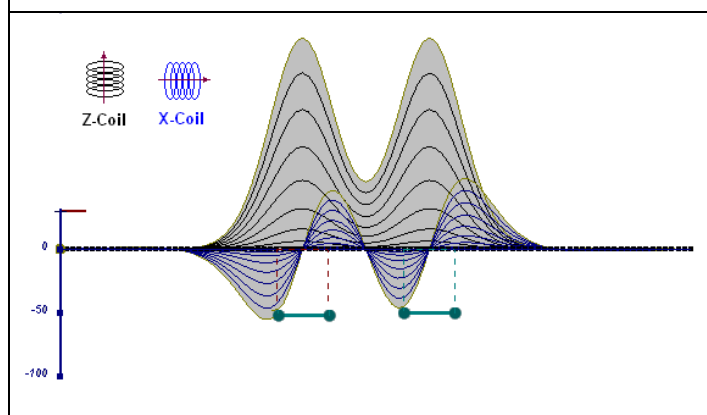


Fig E-14: two horizontal thin plates

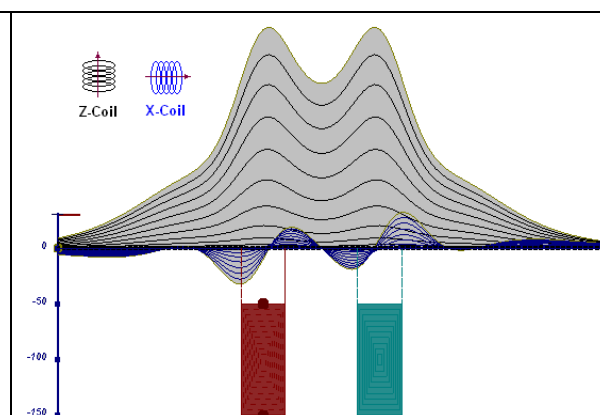


Fig E-15: two vertical thick plates

The same type of target but with different thickness, for example, creates different form of the response:

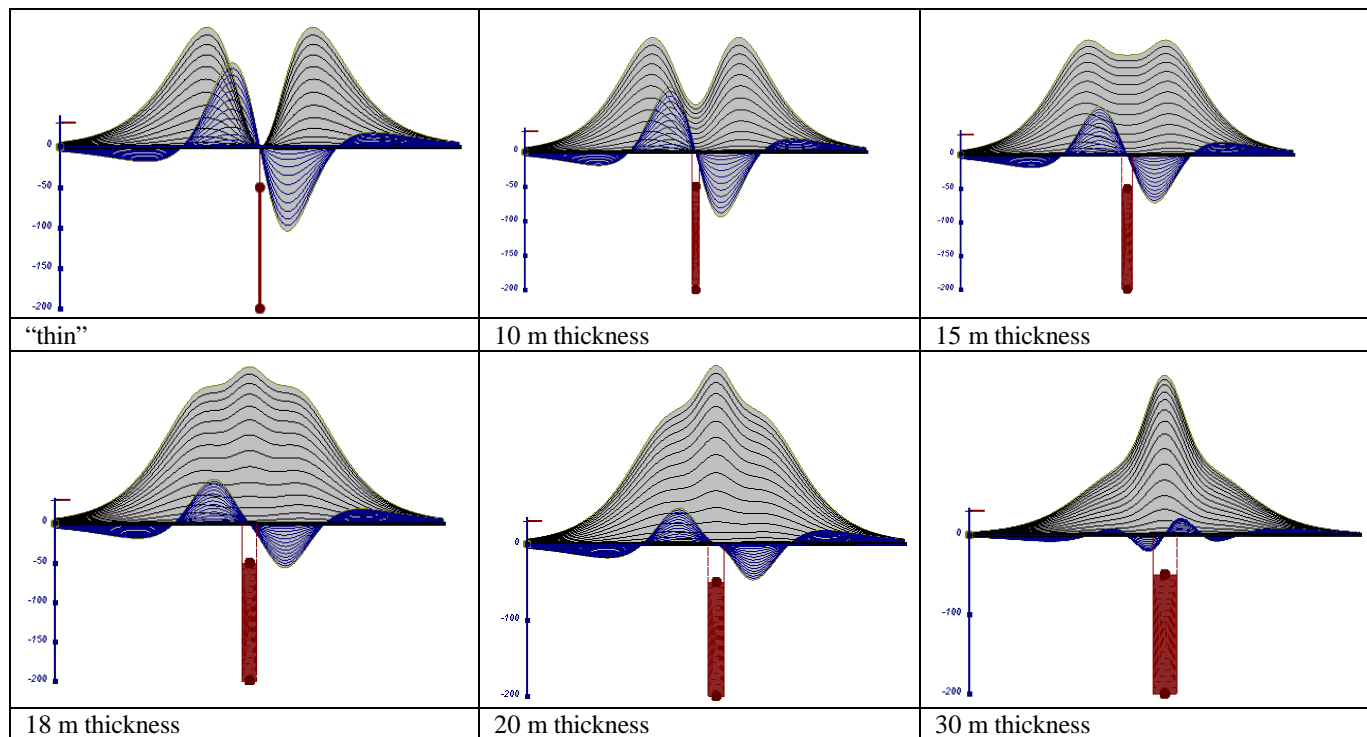


Fig.E-16 Conductive vertical plate, depth 50 m, strike length 200 m, depth extend 150 m.

Alexander Prikhodko, PhD, P.Geol
Geotech Ltd.

September 2010

APPENDIX F EM TIME CONSTANT (TAU) ANALYSIS

Estimation of time constant parameter¹ in transient electromagnetic method is one of the steps toward the extraction of the information about conductances beneath the surface from TEM measurements.

The most reliable method to discriminate or rank conductors from overburden, background or one and other is by calculating the EM field decay time constant (TAU parameter), which directly depends on conductance despite their depth and accordingly amplitude of the response.

Theory

As established in electromagnetic theory, the magnitude of the electro-motive force (emf) induced is proportional to the time rate of change of primary magnetic field at the conductor. This emf causes eddy currents to flow in the conductor with a characteristic transient decay, whose Time Constant (Tau) is a function of the conductance of the survey target or conductivity and geometry (including dimensions) of the target. The decaying currents generate a proportional secondary magnetic field, the time rate of change of which is measured by the receiver coil as induced voltage during the Off time.

The receiver coil output voltage (e_0) is proportional to the time rate of change of the secondary magnetic field and has the form,

$$e_0 \propto (1 / \tau) e^{-(t / \tau)}$$

Where,

$\tau = L/R$ is the characteristic time constant of the target (TAU)

R = resistance

L = inductance

From the expression, conductive targets that have small value of resistance and hence large value of τ yield signals with small initial amplitude that decays relatively slowly with progress of time. Conversely, signals from poorly conducting targets that have large resistance value and small τ , have high initial amplitude but decay rapidly with time¹ (Fig. F1).

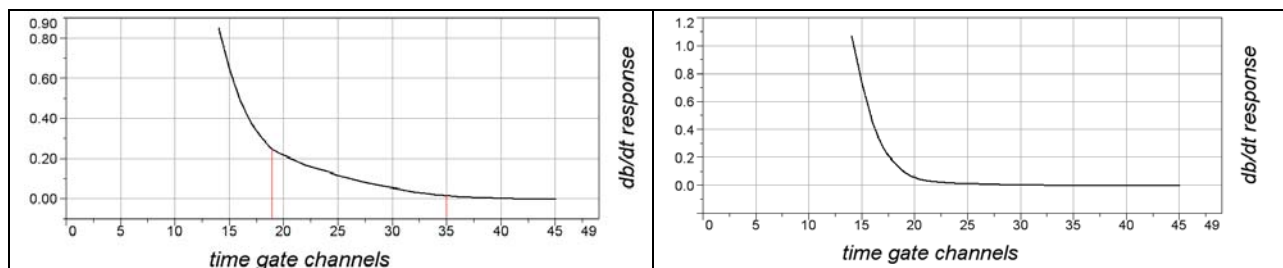


Figure F1 Left – presence of good conductor, right – poor conductor.

¹ McNeill, JD, 1980, “Applications of Transient Electromagnetic Techniques”, Technical Note TN-7 page 5, Geonics Limited, Mississauga, Ontario.

EM Time Constant (Tau) Calculation

The EM Time-Constant (TAU) is a general measure of the speed of decay of the electromagnetic response and indicates the presence of eddy currents in conductive sources as well as reflecting the “conductance quality” of a source. Although TAU can be calculated using either the measured dB/dt decay or the calculated B-field decay, dB/dt is commonly preferred due to better stability (S/N) relating to signal noise. Generally, TAU calculated on base of early time response reflects both near surface overburden and poor conductors whereas, in the late ranges of time, deep and more conductive sources, respectively. For example early time TAU distribution in an area that indicates conductive overburden is shown in Figure 2.

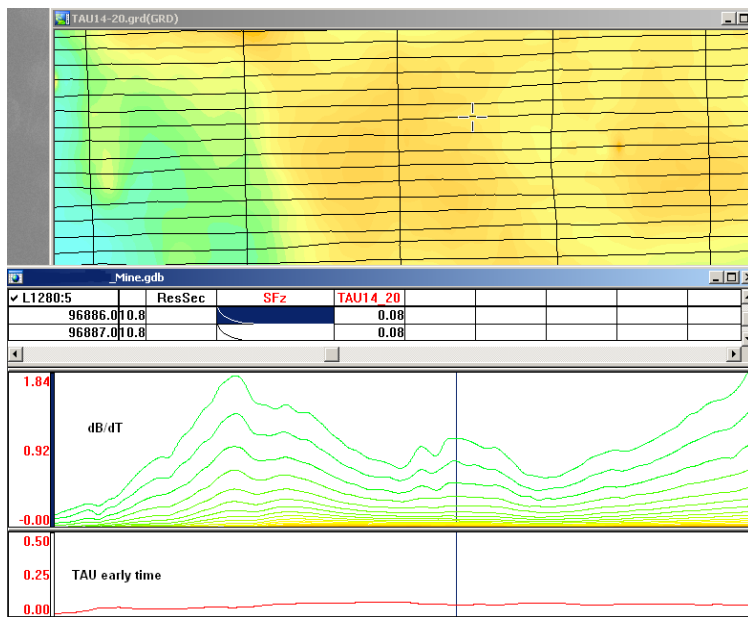


Figure F2 – Map of early time TAU. Area with overburden conductive layer and local sources.

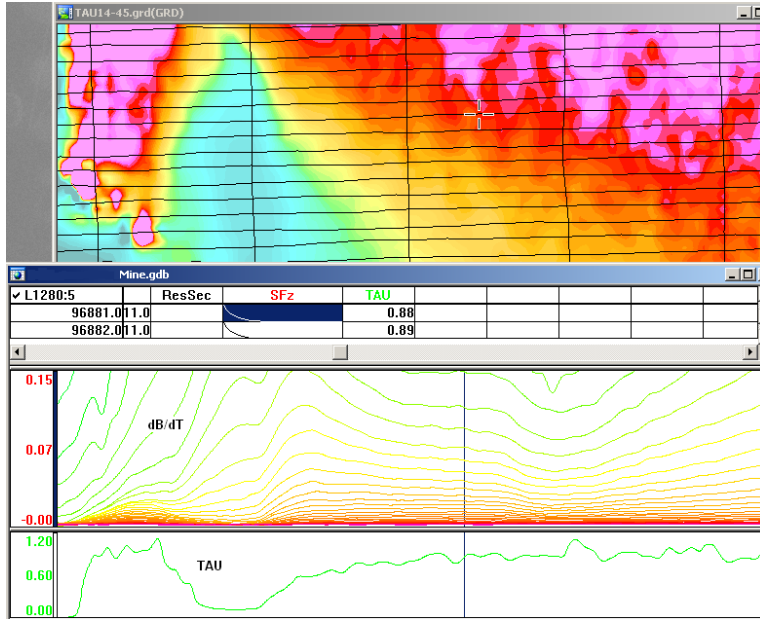


Figure F3 – Map of full time range TAU with EM anomaly due to deep highly conductive target.

There are many advantages of TAU maps:

- TAU depends only on one parameter (conductance) in contrast to response magnitude;
- TAU is integral parameter, which covers time range and all conductive zones and targets are displayed independently of their depth and conductivity on a single map.
- Very good differential resolution in complex conductive places with many sources with different conductivity.
- Signs of the presence of good conductive targets are amplified and emphasized independently of their depth and level of response accordingly.

In the example shown in Figure 4 and 5, three local targets are defined, each of them with a different depth of burial, as indicated on the resistivity depth image (RDI). All are very good conductors but the deeper target (number 2) has a relatively weak dB/dt signal yet also features the strongest total TAU (Figure 4). This example highlights the benefit of TAU analysis in terms of an additional target discrimination tool.

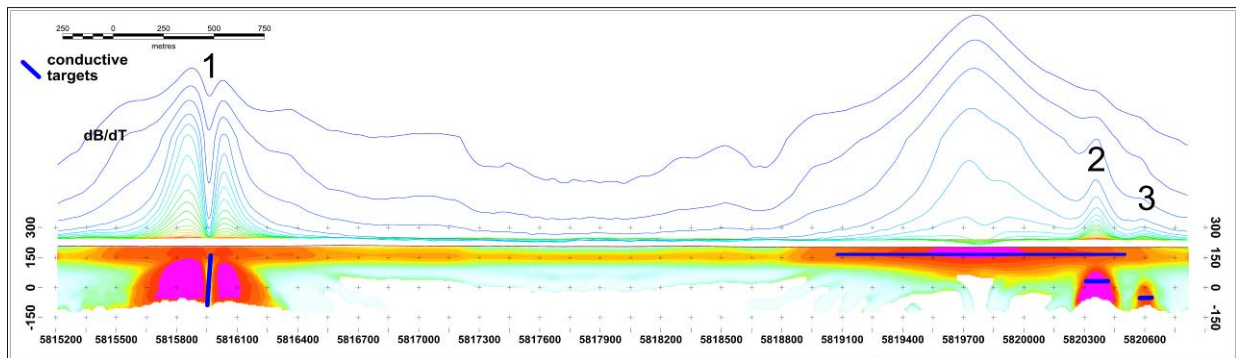


Figure F4 – dB/dt profile and RDI with different depths of targets.

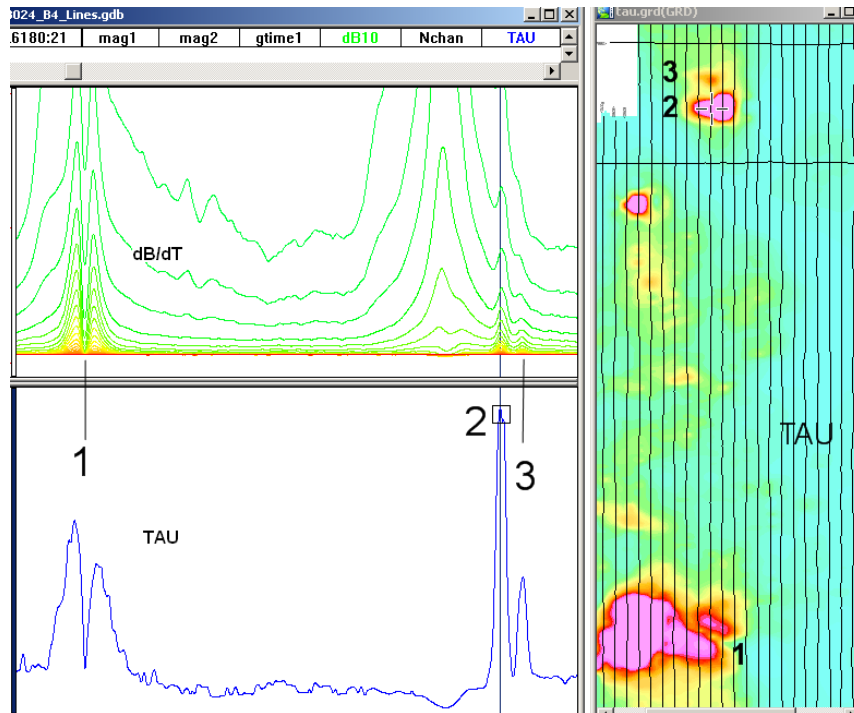


Figure F5 – Map of total TAU and dB/dt profile.

The EM Time Constants for dB/dt and B-field were calculated using the “sliding Tau” in-house program developed at Geotech2. The principle of the calculation is based on using of time window (4 time channels) which is sliding along the curve decay and looking for latest time channels which have a response above the level of noise and decay. The EM decays are obtained from all available decay channels, starting at the latest channel. Time constants are taken from a least square fit of a straight-line (log/linear space) over the last 4 gates above a pre-set signal threshold level (Figure F6). Threshold settings are pointed in the “label” property of TAU database channels. The sliding Tau method determines that, as the amplitudes increase, the time-constant is taken at progressively later times in the EM decay. Conversely, as the amplitudes decrease, Tau is taken at progressively earlier times in the decay. If the maximum signal amplitude falls below the threshold, or becomes negative for any of the 4 time gates, then Tau is not calculated and is assigned a value of “dummy” by default.

² by A.Prikhodko

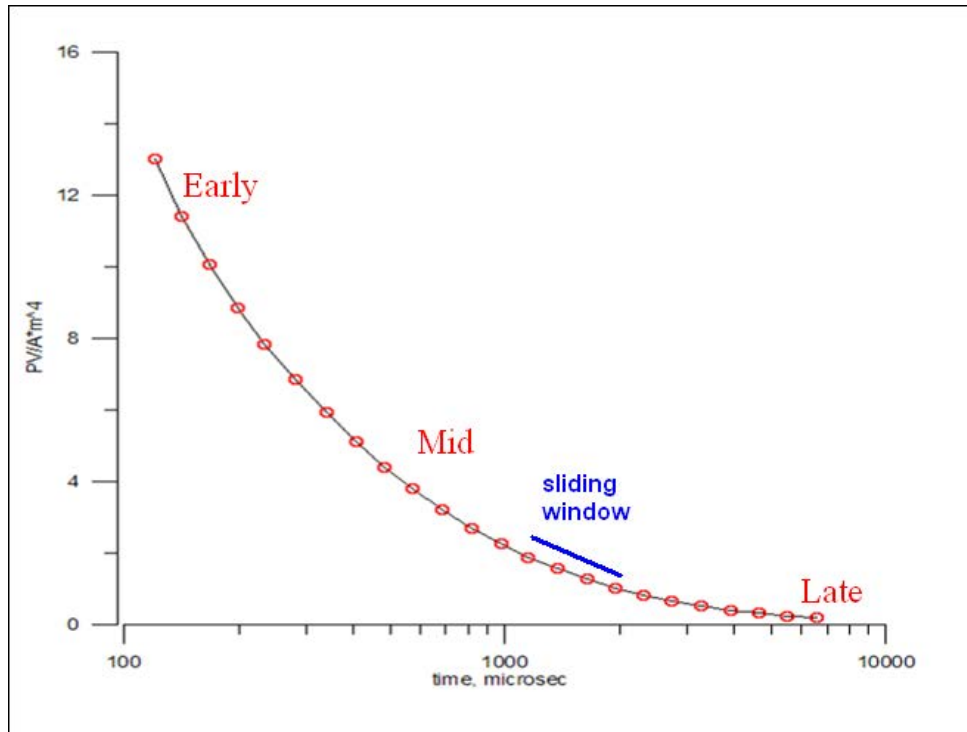


Figure F6 - Typical dB/dt decays of Vtem data

Alexander Prikhodko, PhD, P.Ge
Geotech Ltd.

September 2010

APPENDIX G

TEM Resistivity Depth Imaging (RDI)

Resistivity depth imaging (RDI) is a technique used to rapidly convert EM profile decay data into an equivalent resistivity versus depth cross-section, by deconvolving the system or measured waveforms from the EM data. There are many different schemes to get conductivity/resistivity depth sections from time-domain data. The used RDI algorithm of Resistivity-Depth transformation is based on a scheme of the apparent resistivity transform of Maxwell A. Meju (1998)¹ and TEM response from a conductive half-space adopted for time-domain data and system configuration. The program is in-house developed at Geotech for VTEM data².

The VTEM Resistivity Depth Sections have been checked and proven on several real known targets, results of drilling and synthetic models (Fig. 1-12). Adding individual responses across the profile produces a pseudo 2-dimensional cross-section, called a RDI. RDIs provide reasonable indications of conductor relative depth and vertical extent, as well as accurate 1D layered-earth apparent conductivity/resistivity structure across a VTEM flight line.

Approximate depth of investigation of a TEM system, image of secondary field distribution in half space, effective resistivity, initial geometry and position of conductive targets is the information obtained on the basis of the RDIs.

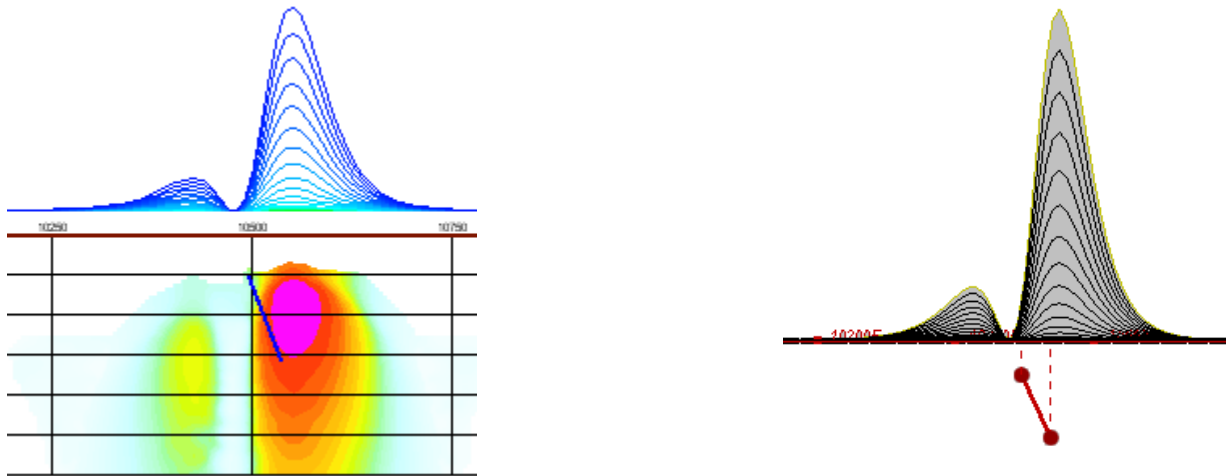


Fig. 1 Maxwell plate model and RDI from the calculated response for conductive “thin” plate (depth 50 m, dip 65 degree, depth extent 100 m).

¹ Maxwell A. Meju, 1998, Short Note: A simple method of transient electromagnetic data analysis, *Geophysics*, **63**, 405–410.

² by A. Prikhodko

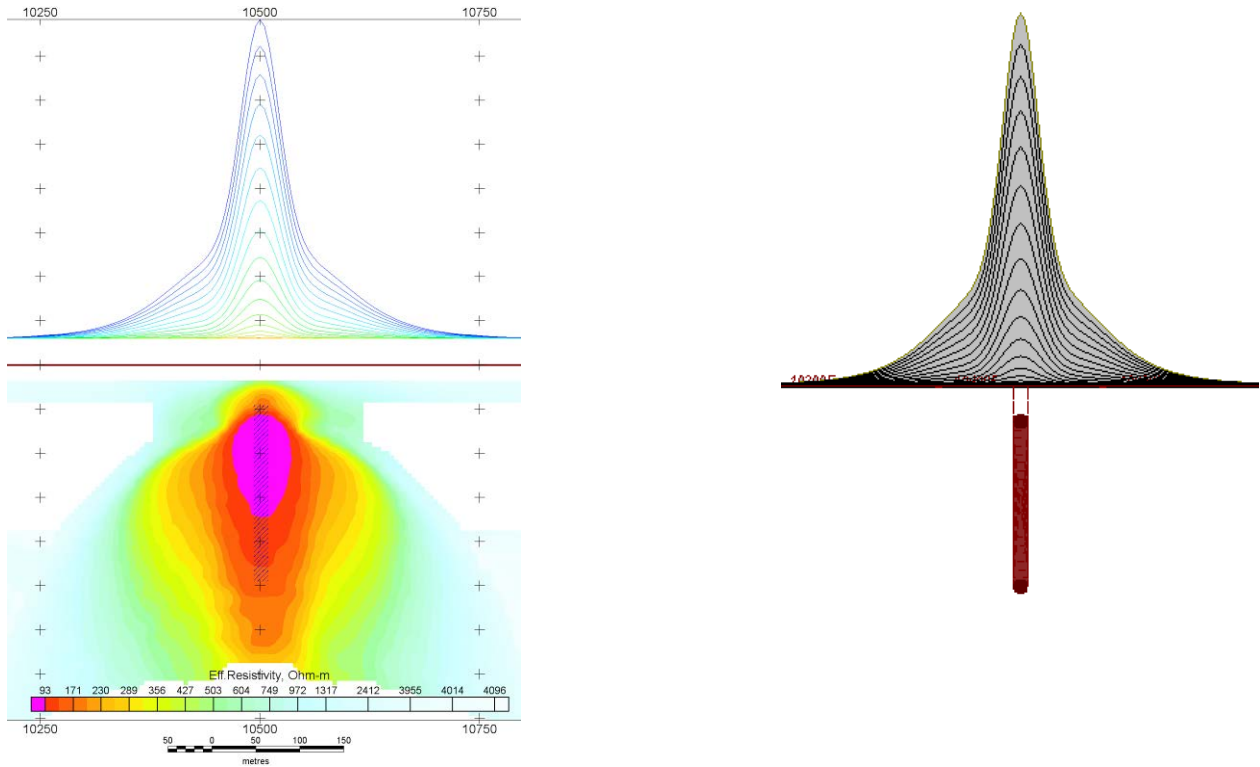


Fig. 2 Maxwell plate model and RDI from the calculated response for “thick” plate 18 m thickness, depth 50 m, depth extend 200 m).

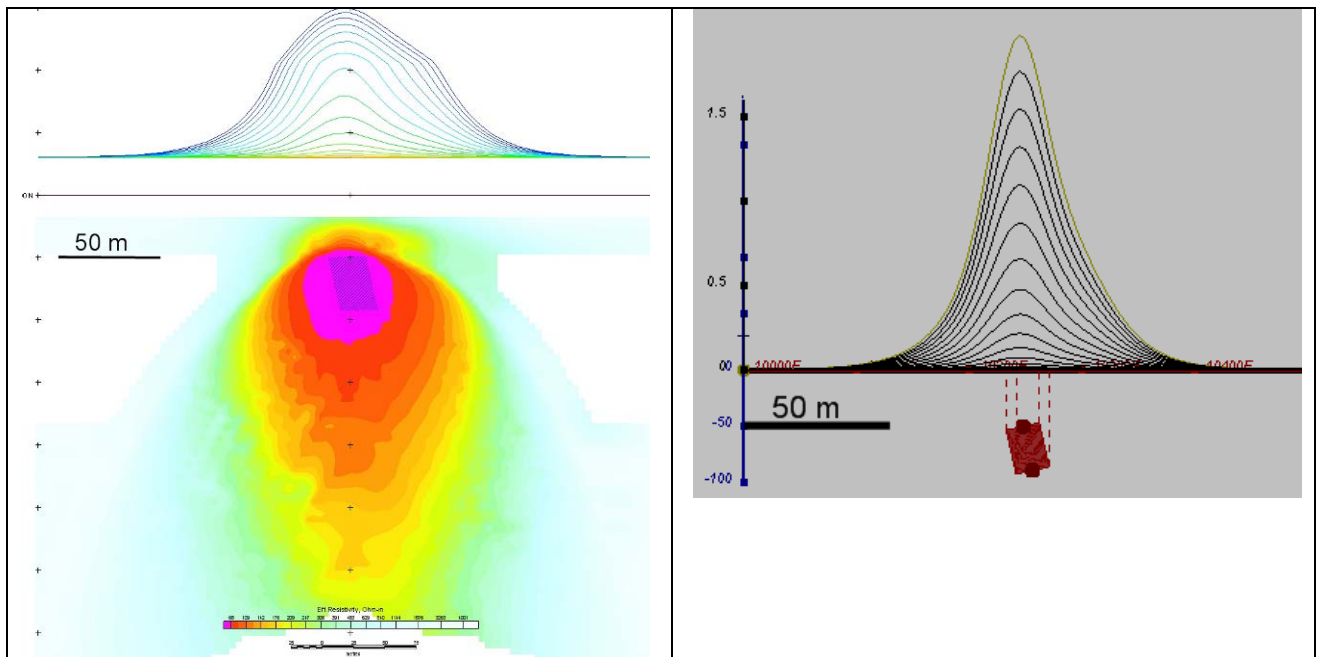


Fig.3 Maxwell plate model and RDI from the calculated response for bulk (“thick”) 100 m length, 40 m depth extend, 30 m thickness

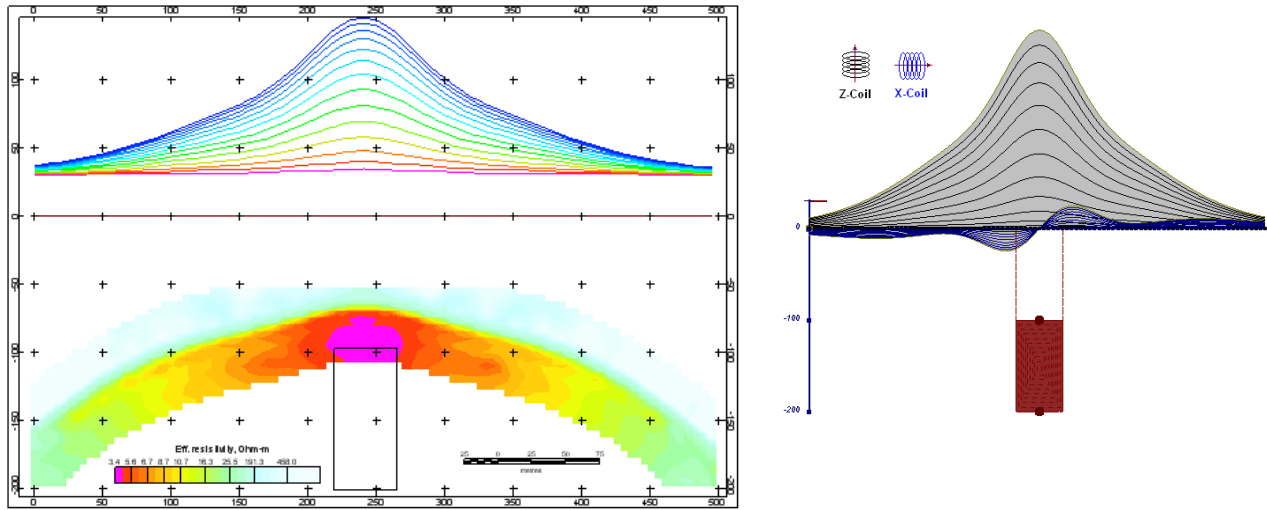


Fig. 4 Maxwell plate model and RDI from the calculated response for “thick” vertical target (depth 100 m, depth extend 100 m). 19-44 chan.

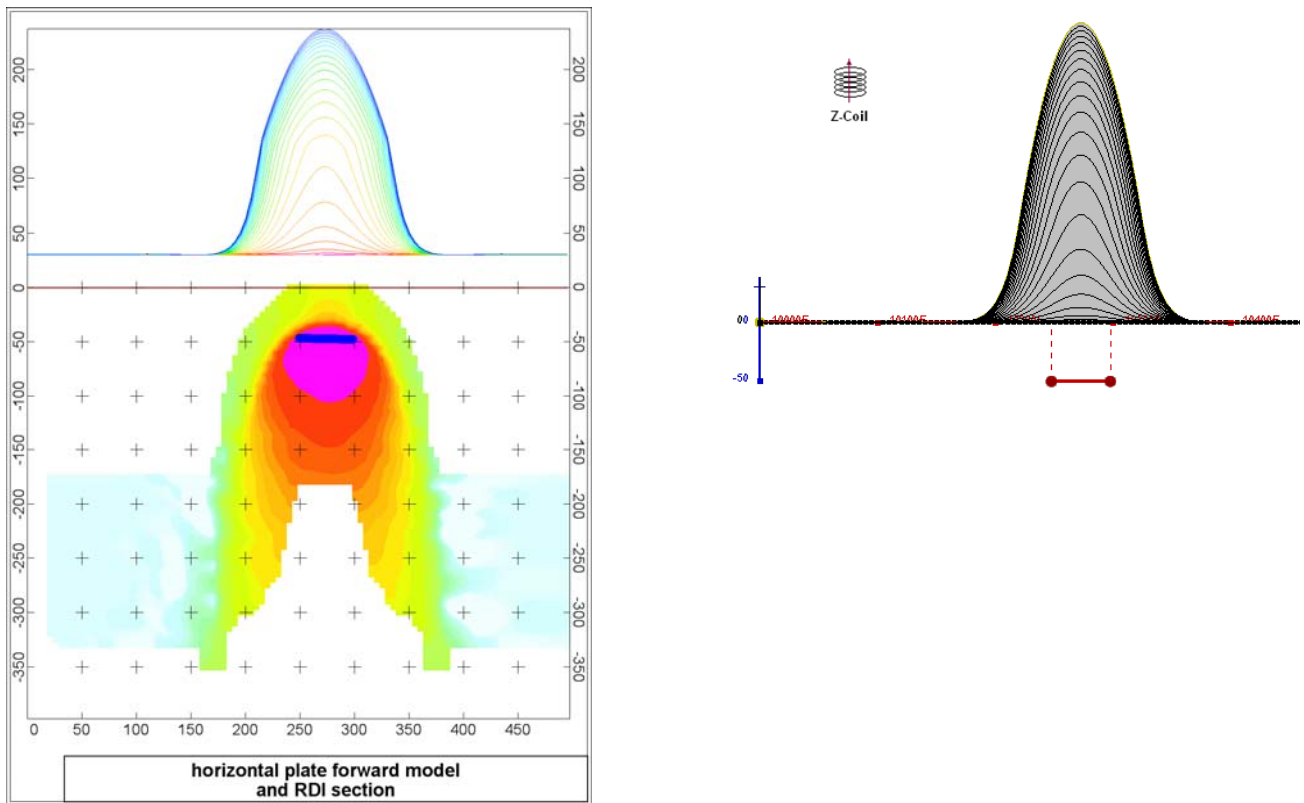


Fig. 5 Maxwell plate model and RDI from the calculated response for horizontal thin plate (depth 50 m, dim 50x100 m). 15-44 chan.

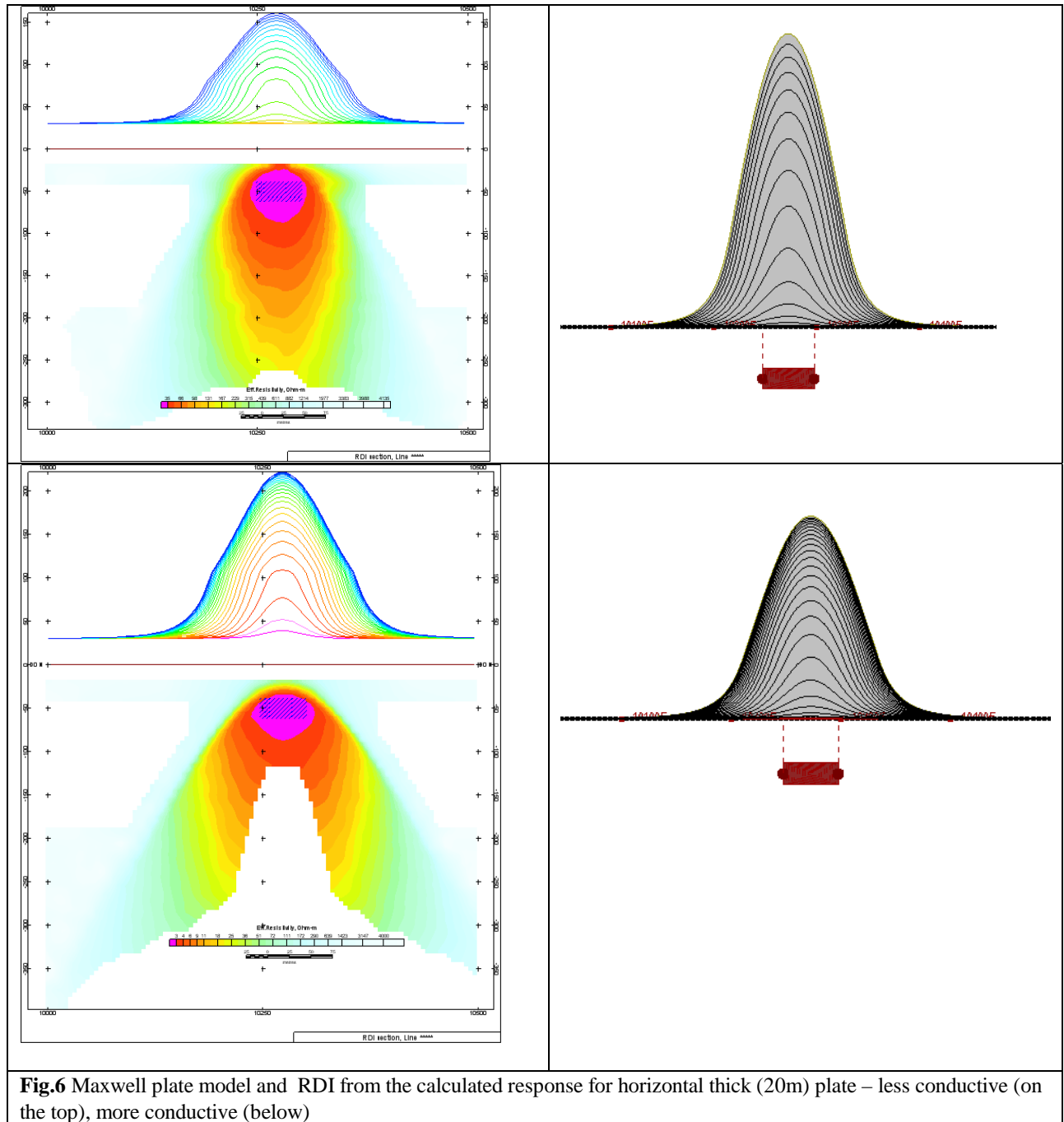


Fig.6 Maxwell plate model and RDI from the calculated response for horizontal thick (20m) plate – less conductive (on the top), more conductive (below)

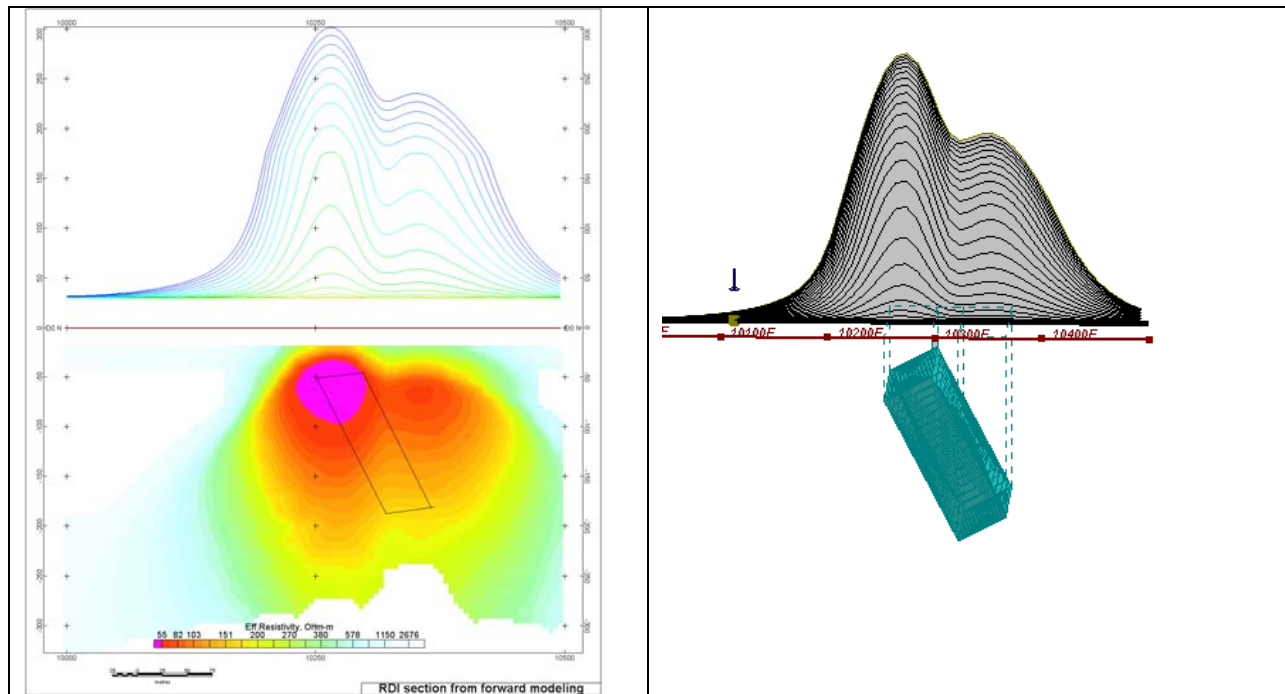


Fig.7 Maxwell plate model and RDI from the calculated response for inclined thick (50m) plate. Depth extend 150 m, depth to the target 50 m.

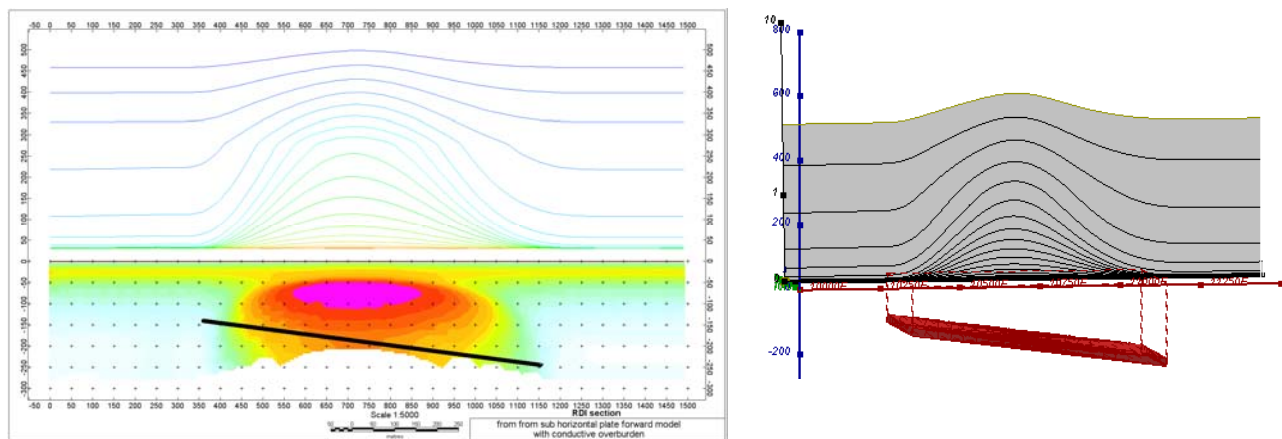


Fig.8 Maxwell plate model and RDI from the calculated response for the long, wide and deep subhorizontal plate (depth 140 m, dim 25x500x800 m) with conductive overburden.

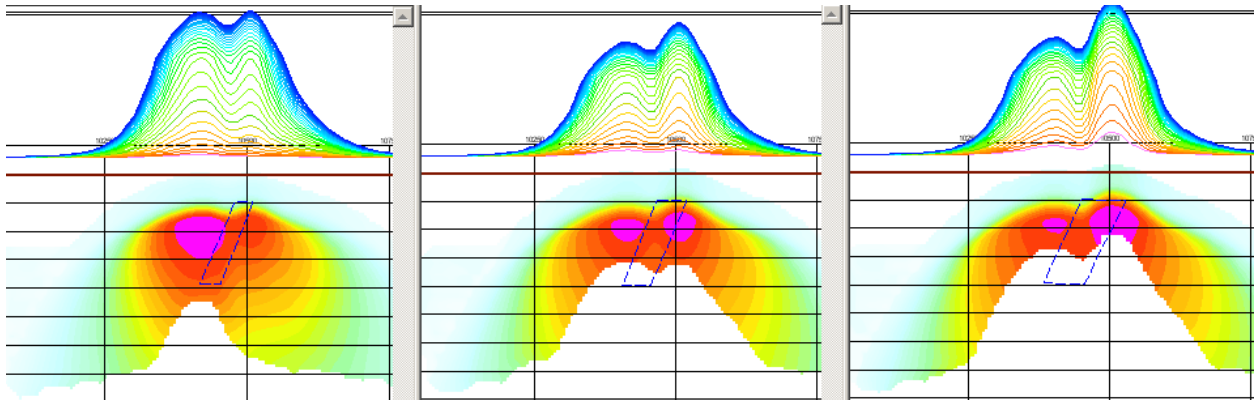


Fig.9 Maxwell plate models and RDIs from the calculated response for “thick” dipping plates (35, 50, 75 m thickness), depth 50 m, conductivity 2.5 S/m.

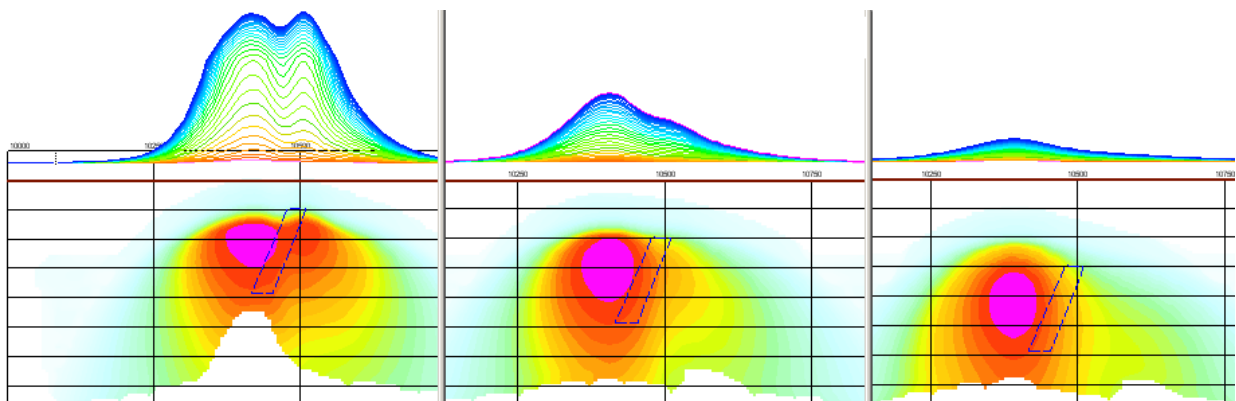


Fig.10 Maxwell plate models and RDIs from the calculated response for “thick” (35 m thickness) dipping plate on different depth (50, 100, 150 m),, conductivity 2.5 S/m.

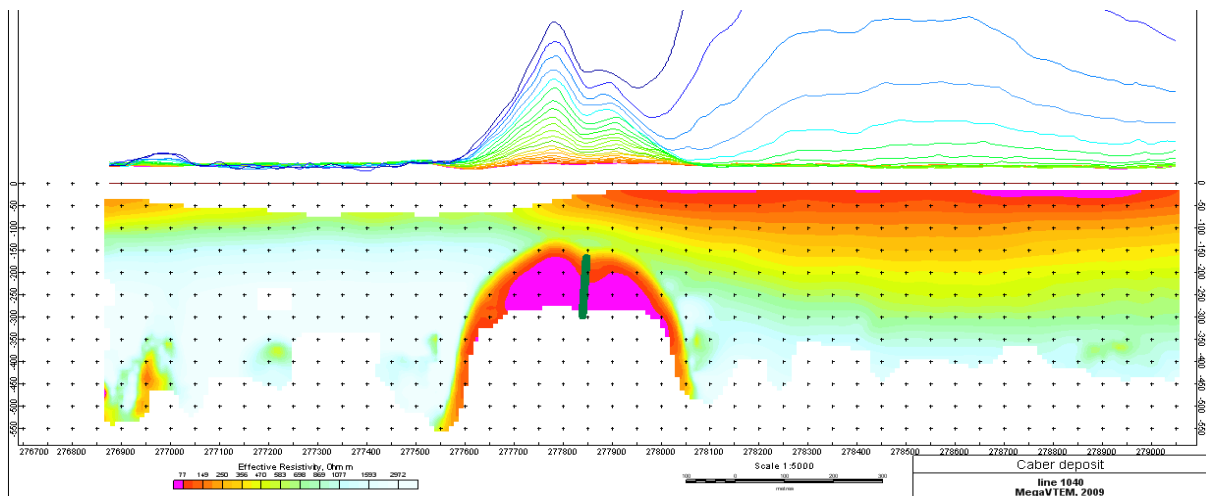


Fig. 11 RDI section of the line over Caber deposit (“thin” subvertical plate target and conductive overburden).

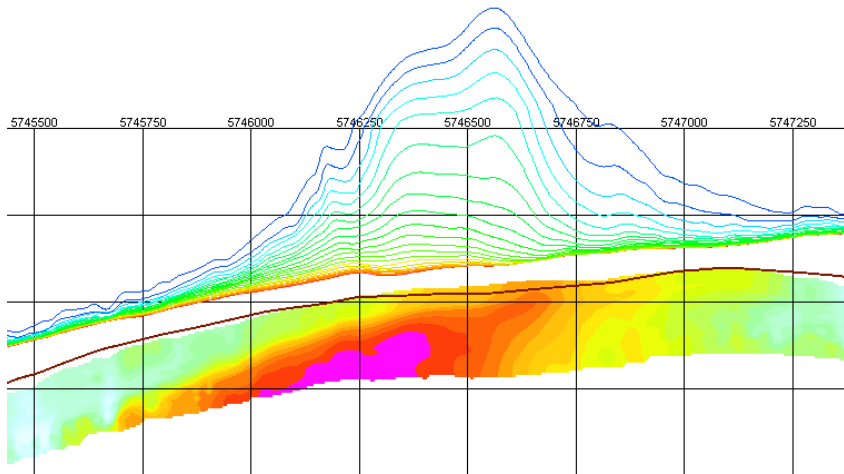
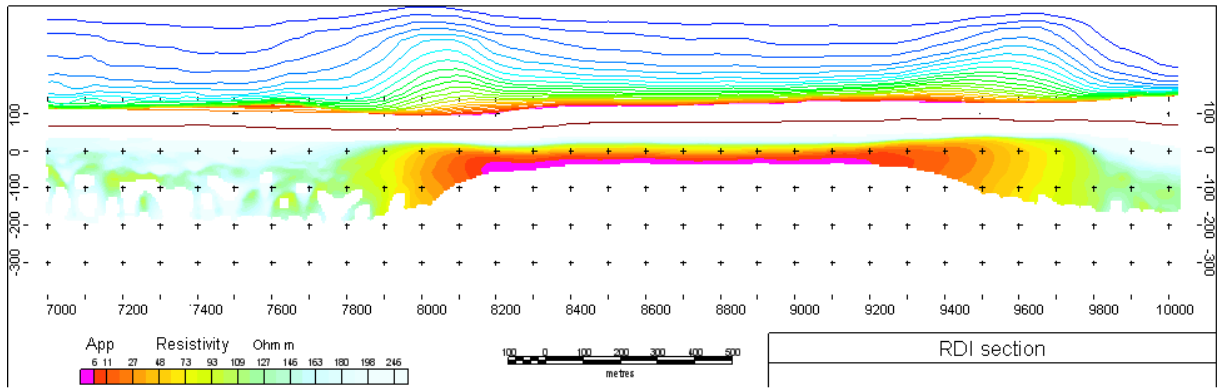
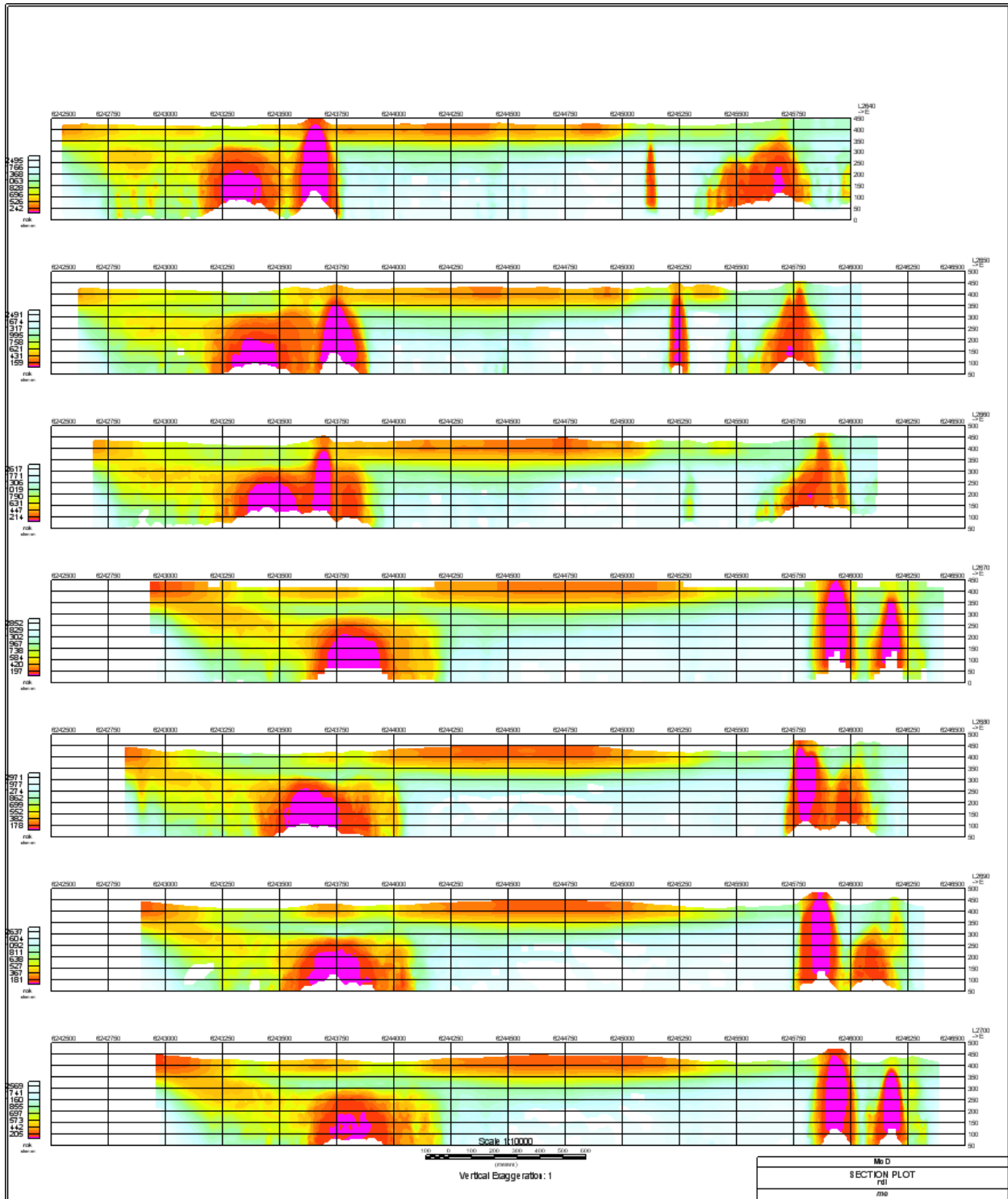
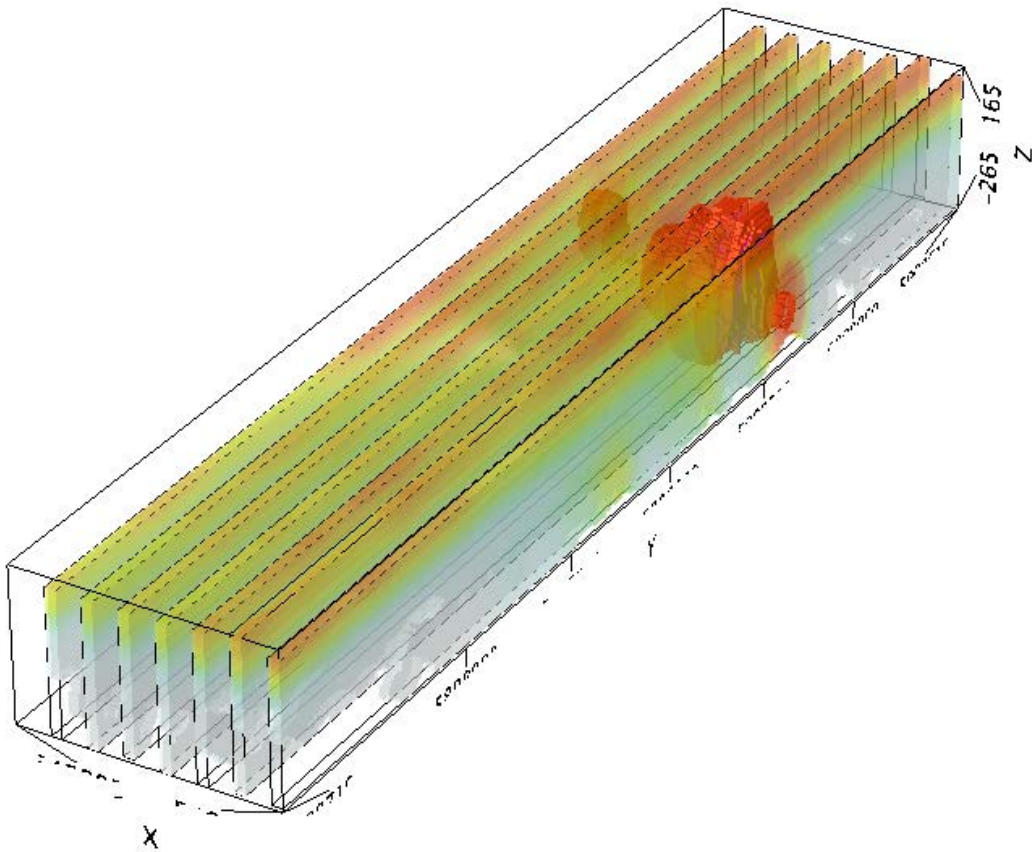
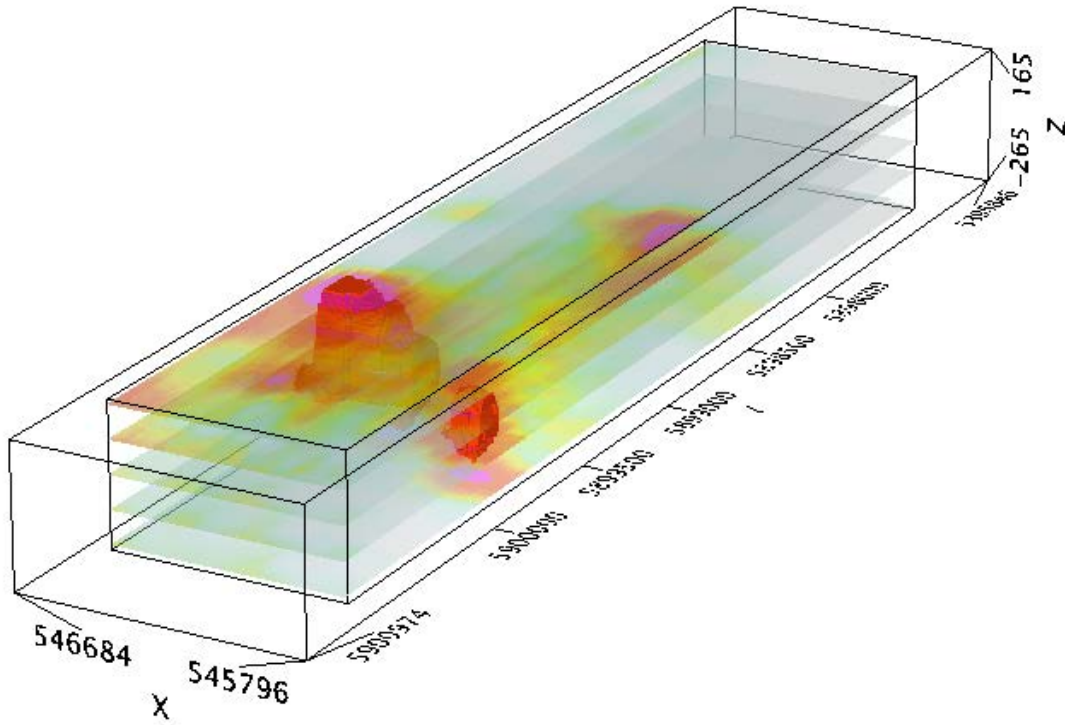


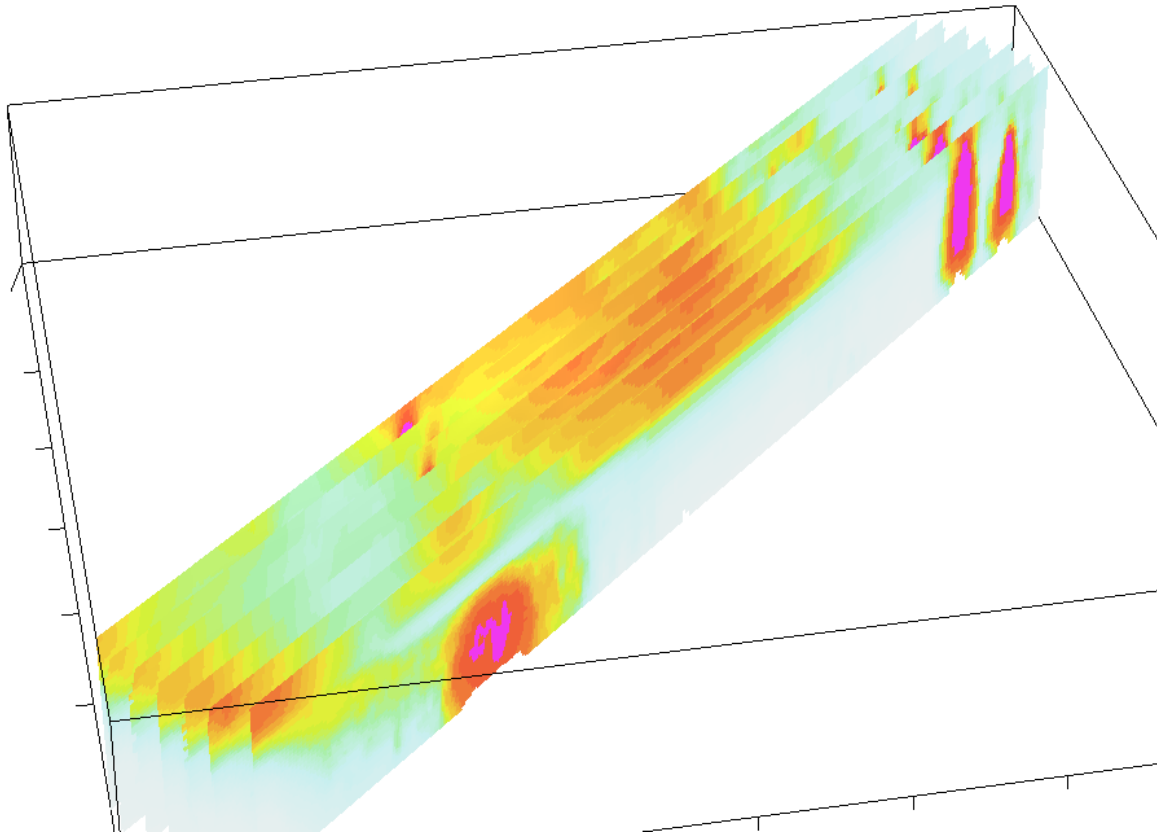
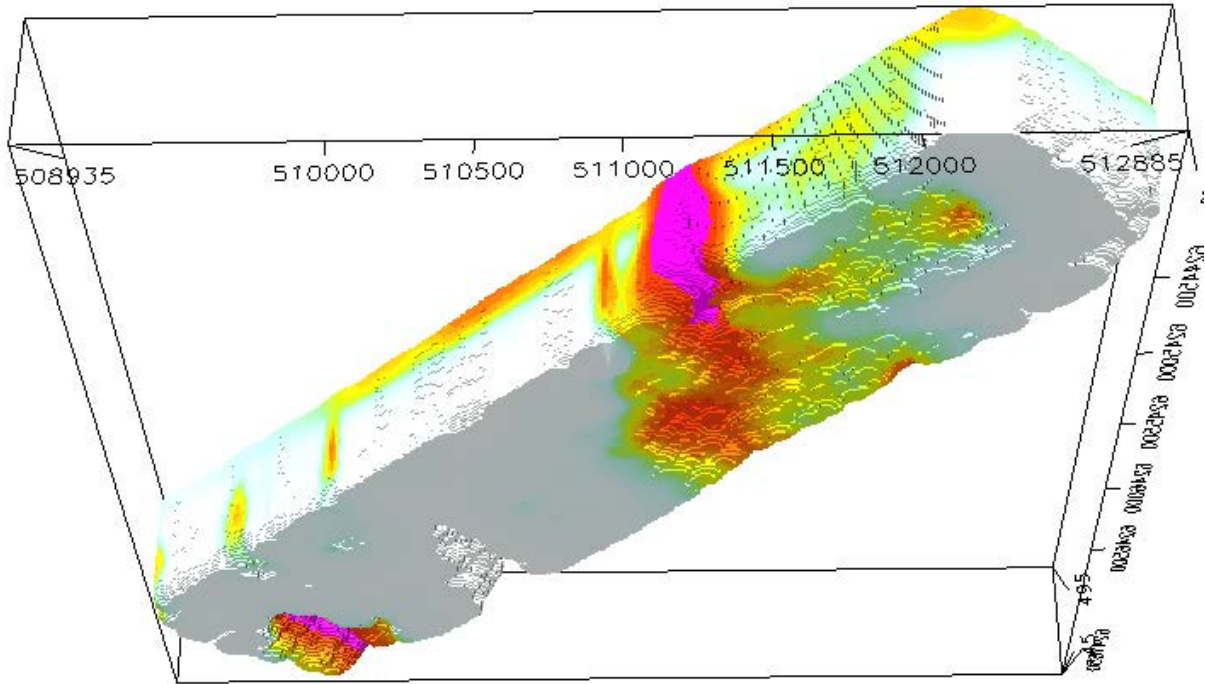
Fig.12 RDI section for the real horizontal and slightly dipping conductive layers

Presentation of series of lines



3d presentation of RDIs





Alexander Prikhodko, PhD, P.Geo
Geotech Ltd.
 September 2010